ABSTRACT

Title of Thesis: MODELING LIQUID EVAPORATION AND USING MOLECULAR DYNAMICS SIMULATION TO ESTIMATE DIFFUSION COEFFICIENTS AND RELATIVE SOLVENT DRYING TIMES

Rehan Choudhary, Master of Science, 2017

Thesis Directed By: Associate Professor and Graduate Program Director, Jeffery Klauda, Department of Chemical and Biomolecular Engineering

In this thesis, the Simultaneous Mass and Energy Evaporation (SM2E) model is presented. This model is based on theoretical expressions for mass and energy transfer and can be used to estimate evaporation rates for pure liquids as well as liquid mixtures at laminar, transition, and turbulent flow conditions. However, due to limited availability of evaporation data, the model has so far only been tested against data for pure liquids and binary mixtures. The model can take evaporative cooling into account. For the case of isothermal evaporation, the model becomes a mass transfer-only model. Also in this thesis, molecular dynamics (MD) simulation is used to estimate gas phase diffusion coefficients based on mean-square displacement methods and results are compared with Chapman-Enksog theory. MD simulation is also used to model evaporation of solvents into air and relative solvent drying times based on simulation are compared with measured values.

MODELING LIQUID EVAPORATION AND USING MOLECULAR DYNAMICS SIMULATION TO ESTIMATE DIFFUSION COEFFICENTS AND RELATIVE SOLVENT DRYING TIMES

by

Rehan Choudhary

Thesis submitted to the Faculty of the Graduate School of the
University of Maryland, College Park, in partial fulfillment
of the requirements for the degree of
Master of Science
2017

Advisory Committee:
Professor Jeffery Klauda, Chair
Professor Panagiotis Dimitrikopoulos
Professor Nam Sun Wang

Acknowledgements

I decided to pursue graduate studies in engineering after having worked in industry and government for about 10 years. In addition to being a son and brother, I was also a husband and father at this point in my life.

We are all influenced by the environments that we are exposed to as we grow and come of age. And from these early years, we carry with us certain habits along with their strengths and weaknesses. But these early years need not determine the remainder of our lives and if we are fortunate, those very same early years will also have equipped us with enough flexibility to understand that we can chart a different path, our own path, if we so choose.

My years as a graduate student were well spent. I didn't just take graduate classes and pursue research endeavors that were already decided for me. I embraced the uncertainty that comes with having to structure your own research and I also used these years to learn how to learn without the structure of a classroom.

I want to express my gratitude to my parents for equipping me with that much needed flexibility during my early years. To my siblings, we are all on our own paths at this point in our lives. It is my hope the aspirations that have driven us apart will also join us once again. To my wife, I am blessed to be walking this path alongside you. And to my children, love and always be kind to your mother and remember that we shall return to God.

There were times when I thought that I may not be able to complete my graduate studies and I am fortunate this is not the case. For this, I want to thank my advisor (Dr. Klauda) for his guidance, patience, and flexibility in working with a part-time graduate student such as myself during these past few years. And I also want to thank Dr. Dimitrikopoulos and Dr. Wang for the enthusiasm they expressed in their willingness to serve on my thesis committee and for reviewing this work.

Table of Contents

List of Tables

List of Figures

Chapter 1: Introduction

Today, whether it be an industrial, commercial, or consumer setting, the use of chemical substances in the liquid state is common practice. These liquid chemicals can be used as reactants, cleaning solvents, coatings, fuels, and additives (Smith, 2001). Liquid chemicals can evaporate and become airborne, which may result in human exposure. Acute (short-term) and chronic (long-term) exposures to hazardous substances may lead to adverse health effects (cancer, non-cancer). Since it is not always possible to measure airborne contaminant concentrations for all relevant exposure scenarios, validated models can be of great help to exposure assessors.

Models based on mass balance principles are commonly used to estimate chemical concentrations in air (Reinke, 1997; Fehrenbacher, et al., 1996; Keil, 2003; Jayjock, et al., 2011). The risk assessment community and certain regulatory agencies routinely make use of such models to assess potential human exposures to volatile liquid substances. In order to estimate these airborne concentrations, one must also have a means of estimating liquid evaporation rates, which are a necessary input for exposure models.

Various models have been developed for estimating evaporation rates (Smith, 2001; Arnold, et al., 2001; Barry, 1995; Braun, et al., 1989; Gajjar, et al., 2013; Hummel, et al., 1996; Mackay, et al., 1973; Nielsen, et al., 1995; Okamoto, et al., 2010; Olsen, et al., 1995). These models are generally used for pure liquids and do not take

evaporative cooling into account, which can overestimate evaporation rates. Some models address evaporation of binary mixtures but assume isothermal conditions (Okamoto, et al., 2010; Olsen, et al., 1995).

One of the objectives of this thesis is to develop an evaporation model that can take evaporative cooling into account, and estimate steady-state evaporation rates for pure liquids as well as liquid mixtures for various flow conditions (laminar, transition, turbulent). The developed model is referred to as the Simultaneous Mass and Energy Evaporation (SM2E) model (Choudhary, 2016). It is based on theoretical expressions for mass and energy transfer, which were refined to optimize agreement with experimental measurements.

Evaporation models generally require input parameters such as vapor pressures, diffusion coefficients, heats of vaporization, and activity coefficients. In some cases, it is possible to find estimates for these parameters from published sources (e.g., publications, property handbooks). However, no such parameters will be available for "new substances" that have not yet been synthesized or introduced into commerce. In such instances, it may be possible to use molecular dynamics (MD) simulation to estimate the required input parameters. It may also be possible to estimate evaporation rates directly from MD simulation.

MD simulations were first conducted in the 1950s (Haile, 1992). These methods are becoming more prevalent due to ongoing computational enhancements and members of the research community are turning to these methods with new

questions and problems. Given a set of initial conditions, MD simulations can be used to compute the movement of individual molecules under the action of forces. If it is possible to simulate motion at the molecular level, then it should be possible to use MD simulation to study molecular diffusion in gases and the evaporation of liquids in air. But if MD simulation is used to estimate diffusion coefficients and relative solvent drying times, how will these estimates compare to results from other theories or experiments?

Various MD simulations have been conducted to study liquid evaporation and diffusion. MD simulation has been used to study the evaporation of liquid argon droplets into argon vapor (Long, et al., 1996) and also liquid xenon droplets into nitrogen gas (Consolini, et al., 2003). The evaporation of a thin layer of liquid water into vacuum was investigated using the TIP4P water model with periodic boundary conditions (PBCs) applied in all Cartesian directions (Yang, et al., 2005). More recently, the evaporation and condensation of thin liquid argon films sandwiched between two solid walls in the Z Cartesian direction with PBCs applied in the X and Y Cartesian directions was also studied (Yu, et al., 2012).

MD simulation has been used to study the diffusion of nitric oxide in liquid water (Zhou, et al., 2005) and also diffusion of hydrogen, carbon monoxide, and water in liquid n-alkanes at elevated temperatures and pressures (Makrodimitri, et al., 2011), where n-alkanes were modeled based on the united-atom Transferable Potentials for Phase Equilibria (TraPPE-UA) and simulation runs were on the order of 30

nanoseconds (ns). Mutual diffusion coefficients for gas mixtures of ethane/nitrogen and n-pentane/nitrogen have been estimated using MD simulation and compared to measured values (Chae, et al., 2011). MD simulation has also been used to study diffusion coefficients of heptane isomers in nitrogen in the range of 500 to 1000 K (Chae, et al., 2011), where results were compared to estimates from Chapman-Enskog (CE) theory and the all-atom Optimized Potentials for Liquid Simulations (OPLS-AA) was used to describe molecular interactions and simulation runs were on the order of 14 ns.

Another objective of this thesis is to use MD simulation to estimate gas phase self and mutual diffusion coefficients using single-particle and collective mean-square displacement (MSD) methods and compare these results to estimates from CE theory. MD simulations will also be used to study the evaporation of liquid solvents into air and relative drying times will be compared with measured values.

Chapter 2: Simultaneous Mass and Energy Evaporation (SM2E) Model

In this chapter, the Simultaneous Mass and Energy Evaporation (SM2E) model is presented. The SM2E model is based on theoretical models for mass and energy transfer. When compared to measured evaporation rates, the theoretical models systematically under or over predicted at various flow conditions: laminar, transition, turbulent. These models were harmonized with experimental measurements to eliminate systematic under or over predictions; a total of 113 measured evaporation rates were used. The SM2E model can be used to estimate evaporation rates for pure liquids as well as liquid mixtures at laminar, transition, and turbulent flow conditions. However, due to limited availability of evaporation data, the model has so far only been tested against data for pure liquids and binary mixtures. The model can take evaporative cooling into account and when the temperature of the evaporating liquid or liquid mixture is known (e.g., isothermal evaporation), the SM2E model reduces to a mass transfer-only model.

2.1 Model Development and Input Parameters

The steady-state evaporation of a liquid is illustrated in **Figure 1**. In this scenario, the air flow over the evaporating liquid is one-dimensional and it is assumed that convection in the x direction is faster than diffusion in the x direction. The velocity profile in the boundary layer is estimated by Equation (1) (Middleman, 1998), where

$v_x(z)$ is the air velocity in the boundary layer in the x direction as a function of z, U_{bulk} is the air velocity outside the boundary layer in the x direction, z is the Z Cartesian coordinate, and δ is the boundary layer thickness. The mean velocity in the boundary layer v_m is given by Equation (2) and it is used to represent the velocity in the boundary layer.

$$v_x(z) = U_{bulk}\left[\frac{2z}{\delta} - \left(\frac{z}{\delta}\right)^2\right] \tag{1}$$

$$v_m = \frac{\int_0^{\delta} v_x(z)\, dz}{\int_0^{\delta} dz} = \frac{2U_{bulk}}{3} \approx 0.67U_{bulk} \tag{2}$$

Figure 1: Steady-state evaporation of a liquid into a flowing stream of air; the presence of a boundary layer is assumed at the liquid-to-air interface; a no-slip condition is applied at $z = 0$; the velocity profile in the boundary layer is parabolic; bottom-side energy transfer is also possible.

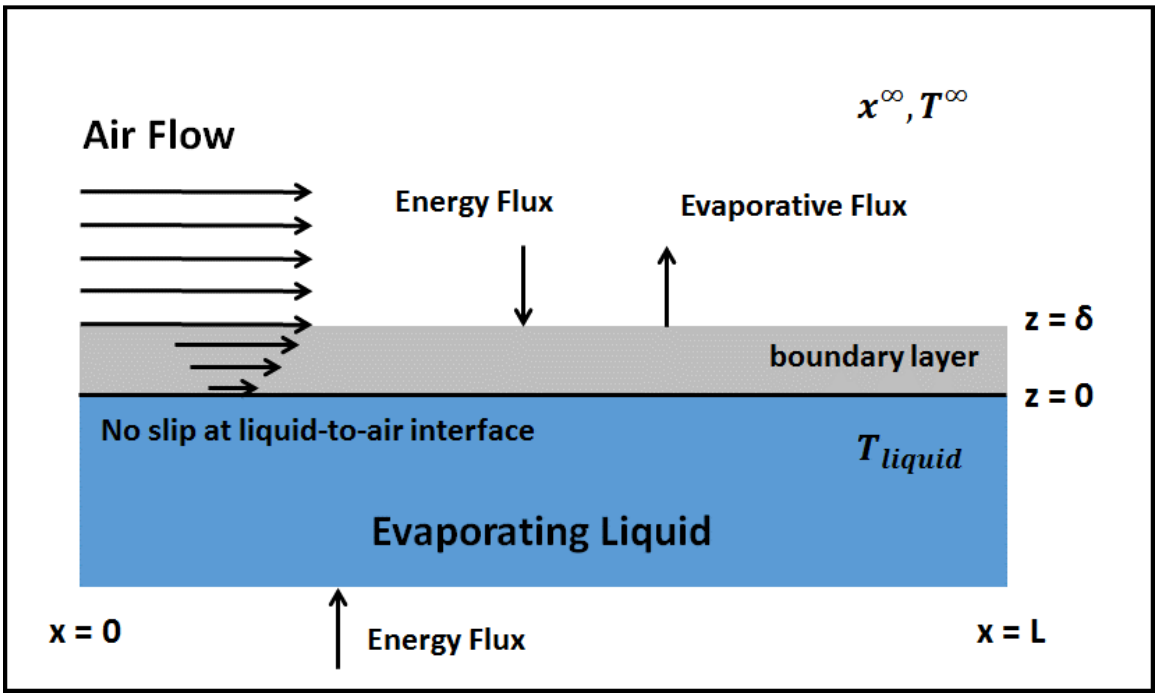

The mass transport equation and relevant boundary conditions are given by Equations (3) and (4), where C_i is the molar concentration of chemical i, C_i^* is the molar concentration of chemical i at liquid-to-air interface, C_i^{∞} is the molar concentration of chemical i far from the liquid-to-air interface, and D_{i-air} is the gas-phase binary diffusion coefficient of chemical i in air.

$$v_m \frac{\partial C_i}{\partial x} = D_{i-air} \frac{\partial^2 C_i}{\partial z^2} \quad \textbf{(3)}$$

$$\begin{aligned} C_i &= C_i^{\infty} \text{ at } x = 0 \\ C_i &= C_i^{*} \text{ at } z = 0 \\ C_i &= C_i^{\infty} \text{ at } z \to \infty \end{aligned} \quad \textbf{(4)}$$

Evaporation produces an outward directed flow of vapor (blowing), which impedes heat transfer to the evaporating liquid and can thus reduce mass transfer compared to mass transfer by just diffusion (absence of blowing) (Middleman, 1998). The mass flux for pure and liquid mixtures with a blowing correction factor (BCF) is given by Equation (5), where ${P_i}^*$ is the partial pressure of chemical i at liquid-to-air interface, ${P_i}^{\infty}$ is the partial pressure of chemical i far from the liquid-to-air interface, ${P_i}^{vap}$ is the vapor pressure of chemical i, P_{total} is the total pressure, R is the gas constant, T_{liquid} is the steady-state temperature of evaporating liquid, x_i is the mole fraction of chemical i in the liquid mixture, ${x_i}^{\infty}$ is the mole fraction of chemical i far from the liquid-to-air interface, n_i is the steady-state mass flux of chemical i, MW_i is the molecular weight of chemical i, K_M is the mass flux correction factor, k_g is the gas-phase mass transfer coefficient, L is the length of the evaporating liquid, γ_i activity

coefficient of chemical i in the liquid mixture, and R_A is a symbol used in the blowing correction factor, $BCF = \frac{\ln[1+R_A]}{R_A}$.

$$
\begin{aligned}
n_i &= -K_M D_{i-air} \left.\frac{\partial C_i}{\partial z}\right|_{z=0} BCF\ MW_i = K_M k_g (C_i^* - C_i^\infty)\, BCF\ MW_i \\
&= K_M k_g \left(\frac{P_i^* - P_i^\infty}{RT_{liquid}} \right) BCF\ MW_i \\
&= K_M \left(\frac{4 D_{i-air} v_m}{\pi L} \right)^{0.5} \left(\frac{x_i P_i^{vap} \gamma_i - P_i^\infty}{R T_{liquid}} \right) \frac{\ln[1+R_A]}{R_A} MW_i
\end{aligned}
\tag{5}
$$

$$
R_A = \left[\frac{\frac{x_i P_i^{vap} \gamma_i}{P_{total}} - x_i^\infty}{1 - \frac{x_i P_i^{vap} \gamma_i}{P_{total}}} \right] \tag{6}
$$

The energy transport equation, relevant boundary conditions, and energy flux are given by Equations (7), (8), and (9), respectively, where k_{air} is the thermal conductivity of air, K_E is the energy flux correction factor, q is the steady-state energy flux due to evaporation, h_g is the gas-phase heat transfer coefficient, T is the air temperature, T^∞ is the air temperature far from the liquid-to-air interface, and α_{air} is the thermal diffusivity of air.

$$v_m \frac{\partial T}{\partial x} = \alpha_{air} \frac{\partial^2 T}{\partial z^2} \quad \textbf{(7)}$$

$$\begin{aligned} T &= T^{\infty} \text{ at } x = 0 \\ T &= T_{Liquid} \text{ at } z = 0 \\ T &= T^{\infty} \text{ at } z \to \infty \end{aligned} \quad \textbf{(8)}$$

$$q = -K_E k_{air} \left.\frac{\partial T}{\partial z}\right|_{z=0} = K_E h_g (T_{liquid} - T^{\infty}) = K_E k_{air} \left(\frac{4 v_m}{\pi L \alpha_{air}}\right)^{0.5} (T_{liquid} - T^{\infty}) \quad \textbf{(9)}$$

The SM2E model is given by Equation (10), where ΔH_i^{vap} is the heat of vaporization of chemical i, n_i and q are obtained from Equations (5) and (9), respectively, and N is the number of chemical substances evaporating, which will be one for a pure liquid. When applicable, the term q_{other} can be used to account for additional routes of energy transfer.

$$\sum_{i=1}^{N} \frac{n_i \Delta H_i^{vap}}{MW_i} = q + q_{other} \quad (10)$$

In this thesis, gas-phase binary diffusion coefficients in air were estimated using Equation (11) (Hummel, et al., 1996), where T_{avg} is the arithmetic mean of T_{liquid} and T^{∞}. Relative to experimental measurements of binary diffusion coefficients in air

(Cussler, 2009), the error in Equation (11) could approximately be ± 18%. The thermal conductivity and thermal diffusivity of air were estimated using Equations (12) and (13), respectively (The Engineering ToolBox, 2014); these equations are valid from -238 ºF to 752 ºF or (123 K to 673 K). The vapor pressure P_i^{vap} of relevant substances was estimated using Equation (14), the Antoine equation. Please refer to **Table 2** for relevant Antoine coefficients and heats of vaporization.

$$D_{i-air}\left(\frac{m^2}{s}\right)=\frac{4.09\text{E-}9*\left[T_{avg}(K)\right]^{1.9}\left[\left(\frac{1}{29}\right)+\left(\frac{1}{MW_i\left(\frac{g}{mol}\right)}\right)\right]^{0.5}\left[MW_i\left(\frac{g}{mol}\right)\right]^{-0.}}{\frac{P_{total}(mmHg)}{760}} \quad \textbf{(11)}$$

$$k_{air}\left(\frac{W}{m-K}\right)=6.952\text{E-}5*T_{avg}(K)+5.392\text{E-}3 \quad \textbf{(12)}$$

$$\alpha_{air}\left(\frac{m^2}{s}\right)=1.363\text{E-}10*\left[T_{avg}(K)\right]^2+5.585\text{E-}8*T_{avg}(K)-6.722\text{E-}6 \quad \textbf{(13)}$$

$$P_i^{vap}(mmHg\text{ or bars})=10^{\left(A-\frac{B}{T_{liquid}(K)-273.15+C}\right)} \quad \textbf{(14)}$$

Activity coefficients (see **Table 1**) for relevant binary mixtures were estimated using XLUNIFAC version 1.0 (Randhol, et al., 2014), a program to calculate activity coefficients of liquids using the UNIFAC model (Fredenslund, et al., 1975). Relative to experimental measurements, the error in the UNIFAC model could approximately be ± 26% (UNIFAC Consortium). The following UNIFAC group-interaction parameters a_{mn} were revised based on more recent updates (Hansen, et al., 1991): $a_{5,22} = 65.28, a_{22,5} = 527.6, a_{9,22} = \text{-}130.3, a_{22,9} = 82.86$

Table 1: UNIFAC activity coefficients for relevant binary mixtures; activity coefficients were estimated at a temperature of 298 K using XLUNIFAC version 1.0 (Randhol, et al., 2014); relative to experimental measurements, the error in the UNIFAC model is approximated to be ± 26% (UNIFAC Consortium); D = dilute component; A = abundant component; x = mole fraction.

Binary Mixtures	**UNIFAC Activity Coefficients**
D: Trichloroethylene, (TCE, x = 10%)	0.67
A: Butyl acetate	0.99
D: 2-Butanone (MEK, x = 10%)	1.27
A: Toluene	1.00
D: Ethanol (x = 10%)	2.06
A: 2-Butanone (MEK)	1.01
D: 2-Butanone (MEK, x = 10%)	2.12
A: Ethanol	1.01
D: Trichloroethylene (TCE, x = 10%)	3.54
A: Ethanol	1.01
D: Ethanol (x = 10%)	4.39
A: Trichloroethylene (TCE)	1.03
D: Ethanol (x = 10%)	3.43
A: Water	1.04

Table 2: Antoine equation coefficients for relevant substances (Knovel, 2013; Poling, et al., 2001); data for Heat of Vaporization (NIST, 2014; Poling, et al., 2001; Smith, et al., 2005); for Xylene, used property values for m-Xylene since commercial Xylene can contain up to 65% m-Xylene (U.S. EPA, 2014) and m-Xylene, o-Xylene, p-Xylene have similar vapor pressures and heats of vaporization.

Substance	A	B	C	Temperature Range (Celsius)	Heat of Vaporization (kJ/mol)
Methanol	8.09126	1582.91	239.096	-98 to 239	37.6
N-propanol	7.77374	1518.16	213.076	-73 to 264	47
1-pentanol	7.21775	1333.96	169.781	-27 to 315	57
Acetone	7.31414	1315.67	240.479	-95 to 235	31.3
Methyl ethyl ketone	7.20103	1325.15	227.093	-85 to 262	34
2-octanone	7.08024	1475.8	178.43	-20 to 351	50.6
Hexane	6.9895	1216.92	227.451	-95 to 234	31
N-heptane	7.04605	1341.89	223.733	-91 to 267	36
Octane	7.14462	1498.96	225.874	-57 to 296	41
Benzene	6.81404	1090.43	197.146	-40 to 289	33.9
Toluene	7.1362	1457.29	231.827	-95 to 319	37
Xylene	7.18115	1573.02	226.671	-48 to 344	41
1-hexanol	7.3423	1538.76	187.498	-45 to 338	61
1-heptanol	7.18822	1482.06	167.773	-34 to 359	67
2-octanol	6.99299	1420.06	165.53	-32 to 364	67.9
Water	8.05573	1723.64	233.076	0 to 374	40.63
Butyl acetate	7.2341	1515.76	222.077	-74 to 307	43
Ethanol	8.13484	1662.48	238.131	-114 to 243	42.3
Trichloroethylene	6.87981	1157.83	202.58	-74 to 298	34.5
Cyclohexane[1]	3.93002	1182.774	220.618	9 to 105	29.97
Diethyl Ether[1]	4.10962	1090.640	231.200	-43 to 55	26.52
n-Pentane[1]	3.97786	1064.840	232.014	-44 to 58	25.79
2-Pentanone[1]	4.15140	1316.730	215.380	10 to 127	33.44

[1] Antoine coefficients for these substances give vapor pressure is in bars, all others give vapor pressure in mmHg.

2.2 Measured Evaporation Rates

The evaporation rate of 16 different liquid chemicals (see **Table 3**) was measured in a test duct; all chemicals were reported as being reagent grade (Braun, et al., 1989). Some details of this study are as follows. A test duct 4 inches in height and 8 inches in width or (10.2 cm x 20.3 cm) was used to measure the evaporation rate of 16 different liquid chemicals from a test pan 1 inch deep by 5.5 square inches or (2.5 cm x 14 cm x 14 cm). Over 150 measurements were made at three conditions of air velocity and air temperature. Air velocities varied from 100 to 1,400 feet per minute (fpm), or 0.51 to 7.11 meters per second. Air temperatures ranged from 40 ^{o}F to 120 ^{o}F, or 4.4 to 48.9 Celsius. The investigators noted that at an air velocity of 100 fpm, the flow in the duct was in the transition region; flow at higher air velocities was turbulent. During evaporation, the base temperature of the test apparatus was controlled to the same temperature that the evaporating liquid reached by evaporative cooling. By attempting to control the base temperature in this fashion, the liquid-to-air interface was expected to be the dominant path for heat transfer. Evaporation rates were determined gravimetrically; as liquid evaporated from the test pan, it was replenished automatically from a supply container to maintain a constant level. The supply container was suspended from a load cell and the evaporation rate was determined from the change in mass of the supply container. The error in evaporation rate measurements was reported as approximately ± 10%. Complete data tables with

measured evaporation rates are included in Appendix A of the study (Braun, et al., 1989).

Table 3: Evaporation rates were measured for 16 different liquid chemicals in a test duct; all chemicals were reported as being reagent grade; evaporation rates were measured gravimetrically (Braun, et al., 1989).

Aliphatic Compounds	Aromatic Compounds	Alcohols		Ketones	Other
Heptane	Benzene	Methanol	1-Hexanol	Methyl Ethyl Ketone	Water
Octane	Toluene	n-Propanol	1-Heptanol	2-Octanone	
Hexane	Xylene	n-Pentanol	2-Octanol	Acetone	

In another study (Olsen, et al., 1995), evaporation rates were measured at a lower air velocity (33 fpm or 0.17 meters per second) while the liquid temperature was actively controlled to approximately 73 ^{o}F (or 22.8 Celsius). Evaporation rates were reported for pure liquids and also for binary mixtures (see **Table 4**); all chemicals were reported as being of high purity (greater than 99.5% by weight). Some details of this study are as follows. A test duct having a square section (0.100 m x 0.100 m) and an evaporation surface length of 0.075 m was used to measure the evaporation rate of pure liquid chemicals and 7 binary liquid mixtures. During evaporation, the temperature of the evaporating liquid was thermostatically controlled to simulate isothermal evaporation. Evaporation rates were determined from the concentration of the evaporating liquid in the effluent air and the total air flow rate; concentrations were measured using an infrared (IR) photo-acoustic detector (Multi-gas Monitor Type

1302). The error in evaporation rate measurements was reported as being less than approximately ± 8%.

Table 4: A total of 17 evaporation rates were reported (Olsen, et al., 1995); four (4) for pure liquids; thirteen (13) for components in binary mixtures; all chemicals were reported as being of high purity (greater than 99.5% by weight); the evaporation rate for Water in the Ethanol/Water binary mixture was not reported; D = dilute component; A = abundant component; x = mole fraction; binary mixtures were maintained at constant composition during testing.

Pure Liquids	Binary Mixtures
2-Butanone	D: Trichloroethylene, (TCE, x = 10%) A: Butyl acetate
Butyl acetate	
Trichloroethylene	D: 2-Butanone (MEK, x = 10%) A: Toluene
Toluene	
	D: Ethanol (x = 10%) A: 2-Butanone (MEK)
	D: 2-Butanone (MEK, x = 10%) A: Ethanol
	D: Trichloroethylene (TCE, x = 10%) A: Ethanol
	D: Ethanol (x = 10%) A: Trichloroethylene (TCE)
	D: Ethanol (x = 10%) A: Water

2.3 Analysis

The theoretical mass and energy transfer models, Equations (5) and (9) with $K_M = 1$ and $K_E = 1$, were first compared to measured values. Next, the correction factors K_M and K_E were optimized to minimize the sum of the squared differences between measured values and model predictions.

Experiments at Transition and Turbulent Flow Conditions

For the evaporation rates measured at transition and turbulent flow conditions, a total of 157 measured evaporation rates were reported (Braun, et al., 1989). Of these reported values, the investigators indicated that a total of six measured values did not meet equilibrium requirements since the measured liquid temperature was higher than the air temperature. These six values were not included in this analysis.

Also, the base temperature of the test apparatus was controlled to the same temperature that the evaporating liquid reached by evaporative cooling. By attempting to control the base temperature in this fashion, the liquid-to-air interface was expected to be the dominant path for heat transfer. However, this control was not ideal in all instances. The absolute difference in liquid and base temperatures ranged from 0 to 17 ^{o}F. Other than its dimensions, not much else is known about the test pan. To ensure that the liquid-to-air interface was the dominant path for heat transfer, in this analysis, only those measured values were used for which the absolute difference in liquid and base temperature was less than 2 ^{o}F. In addition, since temperatures were measured to a tolerance of ±1 ^{o}F, only those values were used for which the absolute difference between liquid and air temperature was greater than 2 ^{o}F.

Based on these data exclusions, the total number of measured values available for model refinements was 96 compared to the original 157; 28 of these 96 values were at an air velocity of 100 fpm (transition flow), while 68 were at air velocities ranging

from 500 to 1,400 fpm (turbulent flow). In the original set of 157 measurements, 43 values were at an air velocity of 100 fpm (transition flow), while 114 were at air velocities ranging from 500 to 1,400 fpm (turbulent flow).

Experiments at Laminar Flow Conditions

For the evaporation rates measured at laminar flow conditions, a total of 17 measured evaporation rates were reported (Olsen, et al., 1995). Since the temperature of the evaporating liquid was actively controlled in these experiments, the available data did not permit estimation of the correction factor K_E for laminar flow conditions. However, the ratio $\frac{K_M}{K_E}$ for the transition and turbulent flow conditions was approximately 0.60. The correction factor K_E for laminar flow conditions was estimated based on the average of this ratio at transition and turbulent flow conditions.

2.4 Results and Discussion

The theoretical and optimized mass transfer models are compared with measured values in **Figure 2** and **Figure 3**, respectively. The theoretical and optimized energy transfer models are compared with measured values in **Figure 4** and **Figure 5**, respectively. Optimized values for the model correction factors at different air flow conditions are presented in **Table 5**. Based on these results, it is evident that different

air flows (laminar, transition, turbulent) affect mass and energy transfer. However, this impact is well within an order of magnitude.

The theoretical mass transfer model seems most appropriate for turbulent flow, while it systematically under and over estimates at transition and laminar flows, respectively. The theoretical energy transfer model is expected to overestimate at laminar flows while it underestimates at transition and turbulent flows. The optimized transfer models eliminate these systematic under and over predictions. For transition and turbulent flows, the correction factor for energy transfer K_E is approximately 60% greater than the correction factor for mass transfer K_M. Transfer coefficients can increase in the transition region due to fast intermixing (Sawhney, 2010); this is supported by the optimized values in **Table 5**.

The goal of this assessment was to start with theoretical expressions for mass and energy transfer and develop the SM2E model. The SM2E model is applicable to laminar, transition, and turbulent flow conditions. When the temperature of the evaporating liquid or liquid mixture is known (e.g., isothermal evaporation), the SM2E model reduces to a mass transfer-only model.

Additional experiments can be performed to further refine the SM2E model. For example, there is a significant need for obtaining and publishing evaporation rates for multi-component mixtures so that models can be validated against a robust data set. Further, the air speed used for laminar conditions (0.17 meters per second) is likely an order of magnitude higher compared to a typical indoor residential environment.

Measuring evaporation rates at lower air speeds (0.01 – 0.02 meters per second) will help to clarify how well the SM2E model performs for indoor residential settings.

Table 5: Optimized model correction factors at different air flow conditions.

Model Correction Factor	Air Flow Condition		
	Laminar	**Transition**	**Turbulent**
K_M	0.4572	1.7497	0.9859
K_E	0.7417	2.7920	1.6264

Figure 2: Theoretical mass transfer model ($K_M = 1$) compared to measured values at various flow conditions (laminar, transition, turbulent).

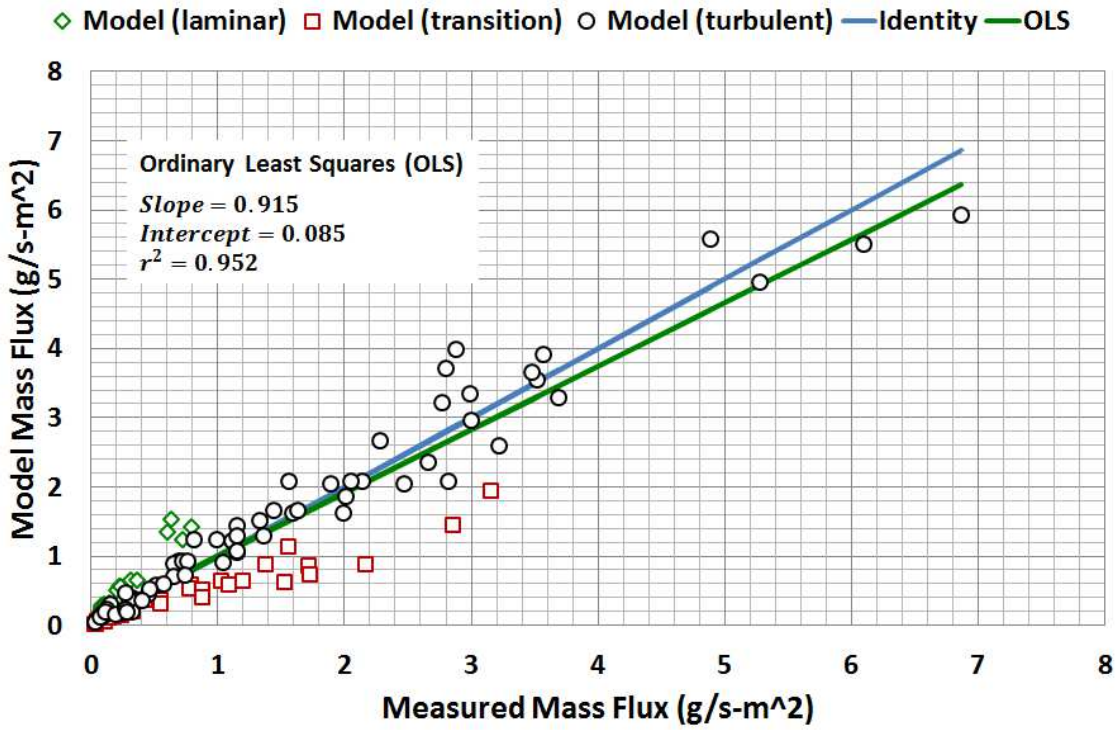

Figure 3: Optimized mass transfer model (K_M) compared to measured values at various flow conditions (laminar, transition, turbulent).

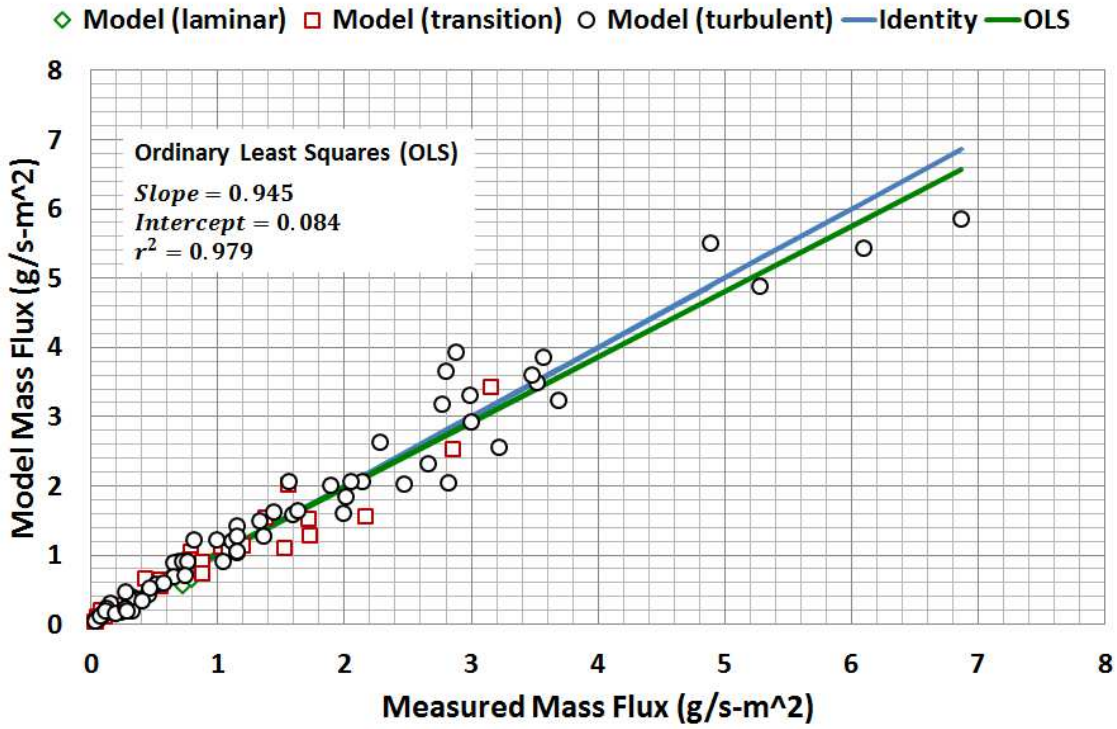

Figure 4: Theoretical energy transfer model ($K_E = 1$) compared to measured values at various flow conditions (transition, turbulent); no data available at laminar flow conditions.

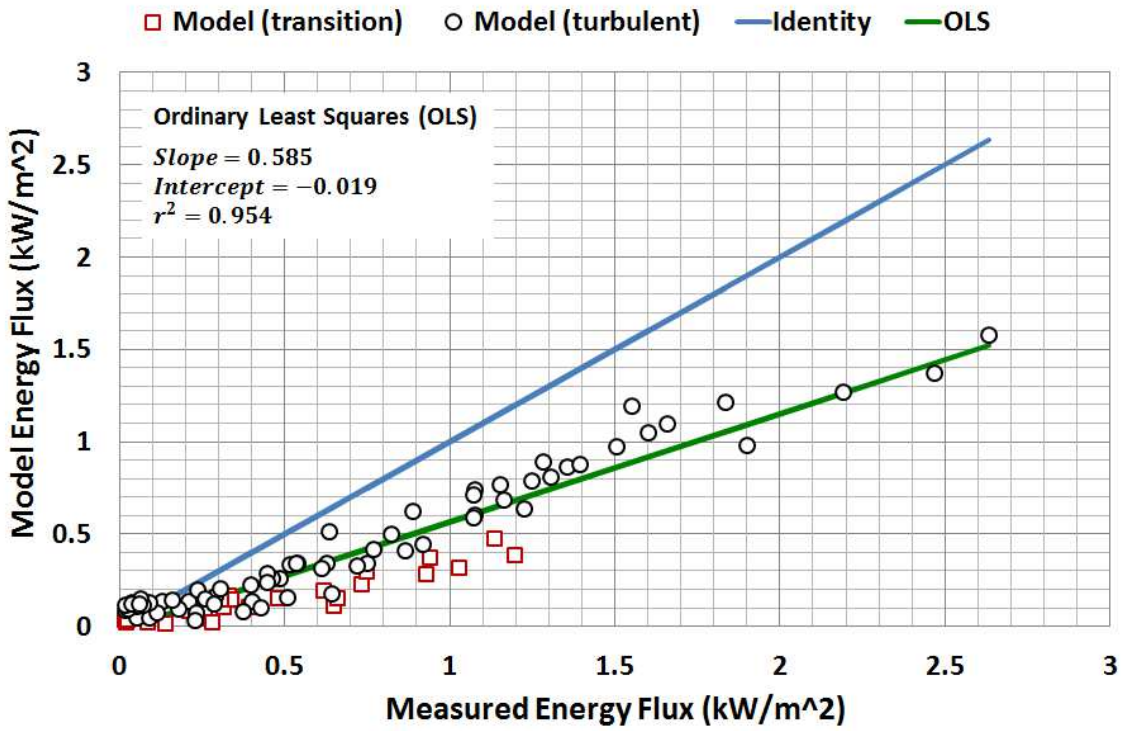

Figure 5: Optimized energy transfer model (K_E) compared to measured values at various flow conditions (transition, turbulent); no data available at laminar flow conditions.

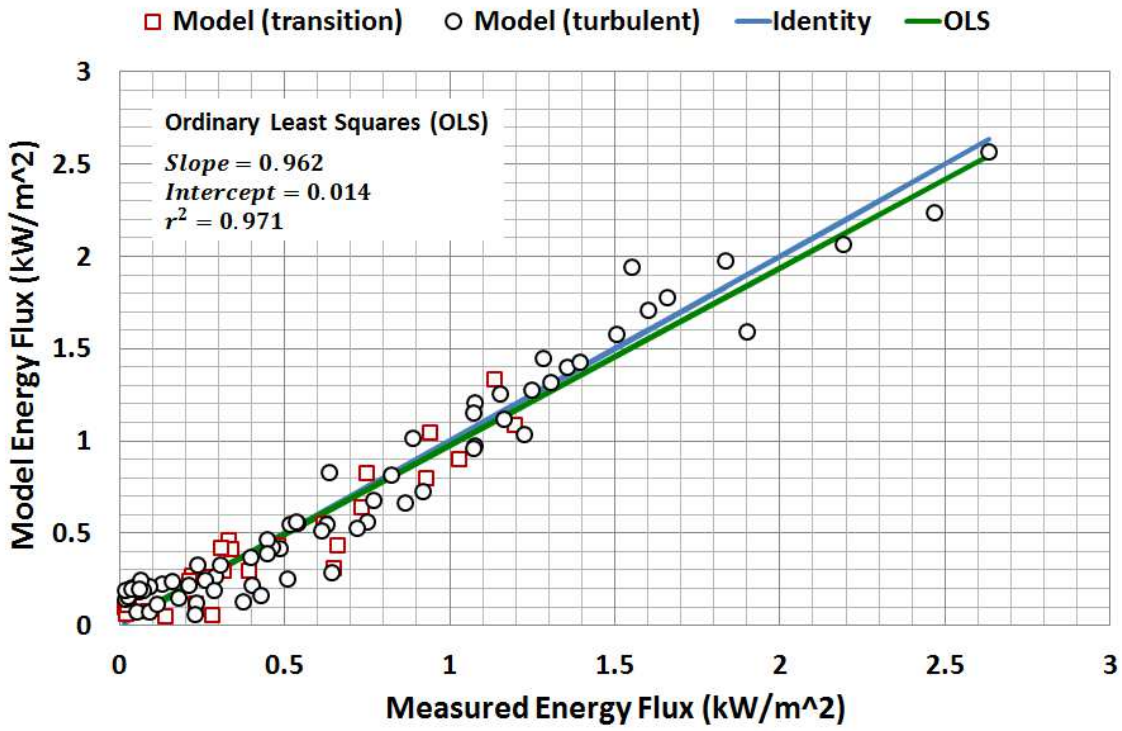

2.5 Conclusions

Based on evaporation experiments reported in the literature, the Simultaneous Mass and Energy Evaporation (SM2E) model was developed. This model was based on theoretical models for mass and energy transfer. These theoretical models were harmonized with experimental measurements at various flow conditions (laminar, transition, turbulent). The SM2E model can be used to estimate evaporation rates for pure liquids as well as liquid mixtures at laminar, transition, and turbulent flow conditions. However, due to limited availability of evaporation data, the model has so far only been tested against data for pure liquids and binary mixtures. The model can take evaporative cooling into account and when the temperature of the evaporating liquid or liquid mixture is known (e.g., isothermal evaporation), the SM2E model reduces to a mass transfer-only model.

Chapter 3: Estimating Transport Properties Using MD Simulation

MD simulation is comprised of developing molecular models and simulating those models (see **Figure 6**). An MD simulation determines molecular trajectories by numerically solving Newton's equations of motion for a system of interacting molecules, where forces between molecules are calculated using a particular form for molecular interactions. These molecular trajectories can then be analyzed to estimate dynamic properties like diffusion coefficients and relative solvent drying times. In this thesis, simulations are conducted using the NAMD MD simulation package (Phillips, et al., 2005). Also, the Transferrable Potentials for Phase Equilibria (TraPPE) (The Siepmann Group, 2015) are used for all chemicals listed in **Table 6**, except water, for which the TIP3P potential is used (Jorgensen, et al., 1983).

Table 6: Coordinate files for these chemicals were obtained from ChemSpider.

2-Pentanone	Benzene	Diethyl Ether	Methanol	Propane
n-Pentane	Carbon Dioxide	Ethanol	Nitrogen	Water
Acetone	Cyclohexane	Methane	Oxygen	

Figure 6: An overview of MD simulation (Haile, 1992).

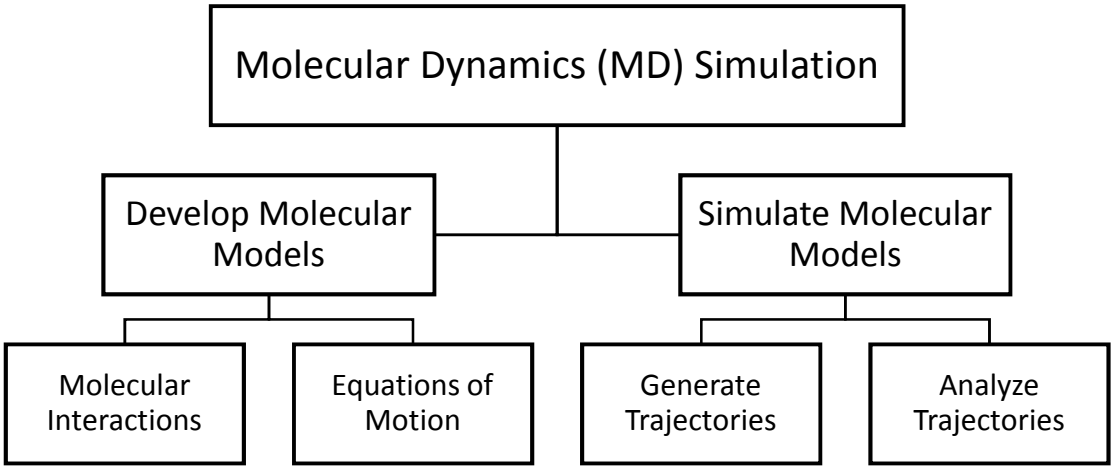

3.1 Equations of Motion

MD simulations are based on Newton's second law. The force exerted on a molecule i is given by Equation (15), where F_i is the force, m_i is the mass, a_i is the acceleration, and r_i is the position:

$$F_i = m_i a_i = m_i \frac{d^2 r_i}{dt^2} \tag{15}$$

The force exerted on a molecule i can also be expressed as the negative gradient of the potential energy V of the system:

$$F_i = -\nabla_i V = -\frac{dV}{dr_i} \tag{16}$$

Equations (15) and (16) can be combined to yield:

$$-\frac{dV}{dr_i} = m_i \frac{d^2 r_i}{dt^2} \tag{17}$$

Given a functional form for the potential energy, and initial positions and velocities for the molecules of the system, Equation (17) can be used to describe the positions, velocities, and accelerations of the molecules as they vary with time.

3.2 Molecular Interactions

The intra- and inter- molecular forces within a system are often represented as a summation of bonded and nonbonded interactions as shown in Equation (18).

$$V(\vec{r}) = \sum V_{bonded}(\vec{r}) + \sum V_{nonbonded}(\vec{r}) \tag{18}$$

3.2.1 Bonded Interactions

Bonded interactions include terms for bond stretching (bonds), angle bending (angles), and bond rotations and out-of-plane bending (dihedrals) (Leach, 2001; The Siepmann Group, 2015):

$$\sum V_{bonded}(\vec{r}) = V_{bonds} + V_{angles} + V_{dihedrals} \tag{19}$$

The first term in Equation (19) models interactions between pairs of bonded atoms and is represented using a Hooke's law formulation as shown in Equation (20), where K_{bond} is the bond constant, r_{ij} is the distance between the bonded atoms, and r_0 is the reference bond length (Leach, 2001; The Siepmann Group, 2015):

$$V_{bonds} = \sum_{bonds} K_{bond}(r_{ij} - r_0)^2 \tag{20}$$

The second term in Equation (19) accounts for the deviation of angles from their reference values (Leach, 2001; The Siepmann Group, 2015). This is also represented using a Hooke's law formulation as shown in Equation (21), where K_θ is the angle constant, θ is the bond angle between atoms A-B-C and is defined as the angle between the bonds A-B and B-C, and θ_0 is the reference bond angle:

$$V_{angles} = \sum_{angles} K_\theta(\theta - \theta_0)^2 \tag{21}$$

The third term in Equation (19) models bond rotations and out-of-plane bending as measured by the angle (dihedral angle) between the planes formed by four consecutively bonded atoms A-B-C-D, where one plane is defined by A-B-C and the second by B-C-D (Leach, 2001; The Siepmann Group, 2015). These types of potentials are represented as a cosine series as shown in Equation (22), where $n + 1$ is the number of terms in the cosine series, K_n are constants, ψ is the dihedral angle as described earlier, and ϕ is the phase shift angle.

$$V_{dihedrals} = \sum_{dihedrals} \sum_{n=0}^{n} K_n[1 + cos(n\psi - \phi)] \tag{22}$$

3.2.2 Nonbonded Molecular Interactions

Nonbonded interactions include terms for van der Waals and electrostatic interactions. These interactions are calculated for pairs of atoms (i, j) that are separated by at least n bonds. Such pairs of atoms (i, j) are said to have a $1, n + 1$ relationship.

$$\sum V_{nonbonded}(\vec{r}) = V_{van\ der\ Waals} + V_{electrostatic} \tag{23}$$

The first term in Equation (23) accounts for van der Waals interactions (Leach, 2001; The Siepmann Group, 2015). It is represented by the Lennard-Jones (LJ) 12-6 potential given by Equation (24), where r_{ij} is the distance between atom pairs (i, j), -ε_{ij} is the minimum potential value, and R_{min} is the distance at which the potential reaches its minimum value:

$$V_{van\ der\ Waals} = \sum_{i=1}^{N} \sum_{j=i+1}^{N} \epsilon_{ij} \left[\left(\frac{R_{min}}{r_{ij}} \right)^{12} - 2 \left(\frac{R_{min}}{r_{ij}} \right)^{6} \right] \quad (24)$$

The second term in Equation (23) accounts for electrostatic interactions and is represented by Coulomb's law as shown in Equation (25), where r_{ij} is the distance between atom pairs (i, j), ε_0 is the permittivity of free space, and q_i is the charge on atom i, and q_j is the charge on atoms j (Leach, 2001; The Siepmann Group, 2015):

$$V_{electrostatic} = \sum_{i=1}^{N} \sum_{j=i+1}^{N} \frac{q_i q_j}{4\pi\varepsilon_0 r_{ij}} \quad (25)$$

3.3 Generate Trajectories

To generate trajectories for molecules in an MD simulation, the equations of motion mentioned in Chapter 3.1 are solved using a finite difference method. These finite difference methods approximate positions and velocities as Taylor series expansions (Leach, 2001). The method used to calculate molecule positions and velocities in NAMD is the velocity Verlet method. Given initial molecule positions and velocities at a time t, the position at some later time $t + \delta t$ is given by:

$$r(t + \delta t) = r(t) + \delta t v(t) + \frac{1}{2}\delta t^2 a(t) \tag{26}$$

With an estimate for the position $r(t + \delta t)$, the acceleration $a(t + \delta t)$ can be derived from the interaction potential given by Equation (18), and then the velocity at some time $t + \delta t$ is given by:

$$v(t + \delta t) = v(t) + \frac{1}{2}\delta t^2 [a(t) + a(t + \delta t)] \tag{27}$$

3.4 Simulation Methodology

In order to prepare, run, and analyze the results of an MD simulation, various software and databases need to be referenced. The basic steps, software, and databases used to perform MD simulations in this work are summarized in **Figure 7**.

Figure 7: Basic steps, software, and databases used to perform MD simulations.

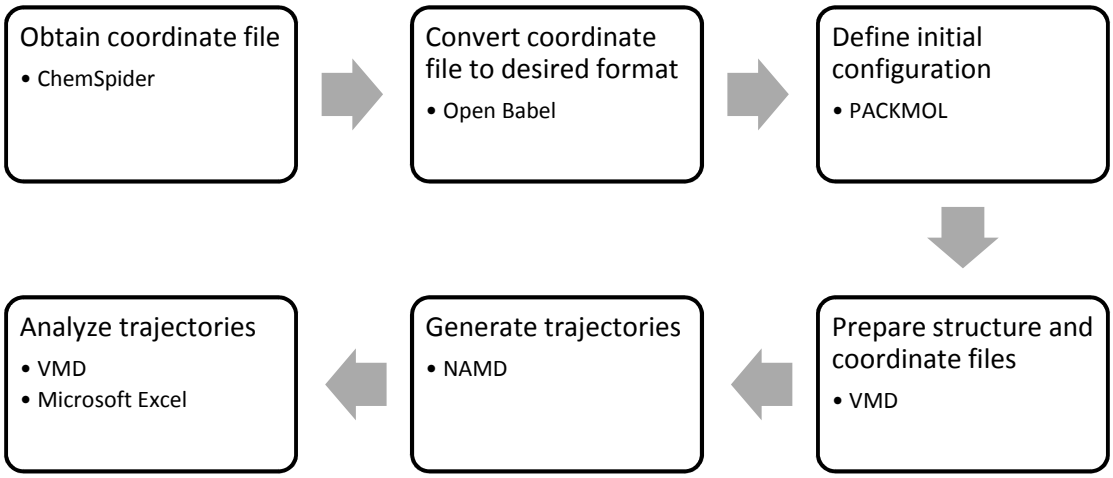

3.4.1 Obtain Coordinate File

In order to compute the movement of individual molecules under the action of forces, it is important to be able to identify the atoms in a particular molecule and their locations in three-dimensional (3D) space. Coordinate files contain just this type of information and are available in many formats. In this work, coordinate files are obtained from ChemSpider (Royal Society of Chemistry, 2015), an online chemical structure database (CSD). The files obtained from ChemSpider use the MDL Molfile

format, which can be identified by the .mol file name extension. Coordinate files were obtained for the chemicals listed in **Table 6**. An example coordinate file can be found in Appendix A: Example MDL Molfile Coordinate File (Methane).

3.4.2 Convert Coordinate File to Desired Format

The coordinate files obtained from ChemSpider are in MDL Molfile format. However, for the MD simulation package used in this work (NAMD), the Protein Data Bank (PDB) format is needed. The PDB file format can be identified by the .pdb file name extension. Chemical file formats were converted from MDL Molfile to PDB using Open Babel (O'Boyle, et al., 2011), a chemical toolbox that can read, write, and convert many different chemical file formats. An example coordinate file can be found in Appendix B: Example PDB Coordinate File (Methane).

3.4.3 Define Initial Configuration

It is important to realize that the coordinate files available thus far only list the atoms and their locations for a particular molecule. However, this work will perform MD simulations for systems that contain many number of molecules in various configurations. So the next step is to define an initial configuration for MD simulation. This is done using PACKMOL (Martinez, et al., 2009), which creates initial configurations (in PDB format) by packing molecules in defined regions of space. Users need only provide coordinate files for each type of molecule, the number of molecules of each type, and the spatial constraints that each type of molecule must

satisfy. Example PACKMOL input files used to prepare initial configurations for this work can be found in Appendix C: Example PACKMOL Configuration Files.

3.4.4 Prepare Structure and Coordinate Files

Now that an initial configuration PDB file has been prepared using PACKMOL, the next step is to prepare a final PDB configuration file and also a Protein Structure File (PSF). Whereas NAMD obtains coordinates from the PDB configuration file, structural information such as bonding is obtained from the PSF file.

Before the PDB configuration file can be finalized and a PSF file created, a force field topology file is needed. This file contains information regarding atom types, charges, and how atoms in a molecule are connected. The topology file used for this work can be found in Appendix D: NAMD Topology File.

Once a topology file is available, Visual Molecular Dynamics (VMD) (Humphrey, et al., 1996), a molecular visualization program, is used to prepare a PSF file and also finalize the PDB configuration file. An example VMD script file used to prepare PSF files and finalize PDB configuration files for this work can be found in Appendix E: Example VMD Script File Used to Prepare PSF and Final PDB.

What does it mean to finalize the PDB file? For example, a Methane molecule is comprised of one Carbon atom bonded to four Hydrogen atoms. The Methane PDB file (see **Table B - 1**) was used to prepare an initial configuration using PACKMOL (see **Table C - 1**). For this work, molecular interactions (see Chapter 3.2) are modeled

using the Transferrable Potentials for Phase Equilibria (TraPPE) for all chemicals listed in **Table 6**, except Water, for which the TIP3P potential is used. The TraPPE potential used for Methane does not model the Hydrogen atoms explicitly, but rather it models Methane as a pseudo CH4 atom. Thus, the initial configuration file is finalized by removing the Hydrogen atoms from the Methane molecules (see **Table E - 1**).

3.4.5 Generate Trajectories

Running an MD simulation using NAMD requires a PDB configuration file, PSF file, force field parameter file, and a configuration file. The PDB configuration and PSF files were described previously and are obtained using VMD (see Chapter 3.4.4).

The parameter file contains the inputs needed to describe the bonded and nonbonded interactions described in Chapter 3.2. As indicated previously, for this work, the Transferrable Potentials for Phase Equilibria (TraPPE) are used for all chemicals listed in **Table 6**, except Water, for which the TIP3P potential is used. The parameter file used for this work can be found in Appendix F: NAMD Parameter File.

A configuration file instructs NAMD on how to run an MD simulation and specifies the various options available in NAMD. Example configuration files used for this work can be found in Appendix G: Example NAMD Configuration Files.

MD simulations for estimating diffusion coefficients were performed with 2 femtoseconds (fs) time-steps, while MD simulations for estimating evaporation were

performed using 0.5 fs time-steps. A smaller time-step was needed for evaporation simulations to ensure simulation stability; errors related to atoms moving too fast were encountered at larger time-steps. The van der Waals forces were force-switched to zero over a range of 12-14 Å. Particle Mesh Ewald was used to include long-range electrostatic interactions with an interpolation order of 4 and a direct space tolerance of 10^{-6}. Langevin dynamics was used to maintain constant temperature. For estimating diffusion coefficients, coordinates were saved every 0.2 picoseconds (ps), while they were saved every 0.8 ps for estimating evaporation. Parameters specific to a particular simulation, such as cell size, temperature, and number of molecules are listed in **Table 7**, **Table 8**, and **Table 9**.

3.4.6 Analyze Trajectories

MD simulations generate trajectories or configurations that are connected in time and they can be used to estimate time-dependent properties such as diffusion coefficients and relative solvent drying times. NAMD produces trajectory files, in DCD file format, that can be analyzed to estimate equilibrium and non-equilibrium properties. For this work, MD simulation trajectories were analyzed using VMD and Microsoft Excel. VMD script files were used to generate relevant information which was then imported into Microsoft Excel for additional data analysis and visualization. Example VMD script files used for this work can be found in Appendix H: Example VMD Script Files for Trajectory Analysis.

3.4.6.1 Diffusion Coefficients

Transport coefficients can be estimated using a time correlation function, but they can also be estimated using mean-square displacement (MSD). The mean-square displacement and time correlation function are related as shown in Equation (28), where D is a transport coefficient, d is the dimensionality (d = 1, 2, 3), t is the time delay, A is a dynamic quantity, and $\dot{A}$ is the time derivative of the dynamic quantity (Haile, 1992):

$$\frac{MSD}{2td} = \frac{\langle [A(t) - A(0)]^2 \rangle}{2td} = D = \frac{1}{d}\int_0^\infty \langle \dot{A}(t)\dot{A}(0) \rangle dt \qquad (28)$$

For the case of one dimensional motion ($d = 1$), the self-diffusion coefficient can be estimated from the single particle MSD as follows:

$$D_{self} = \left[\frac{\langle [z_i(t) - z_i(0)]^2 \rangle}{2t}\right] = \frac{MSD_{single-particle}}{2t} \qquad (29)$$

The three dimensional (d = 3) mutual diffusion coefficient can be estimated using the following time correlation function, where D_{12} is the mutual diffusion coefficient, N is the total number of molecules, N_1 is the number of molecules of species 1, N_2 is the number of molecules of species 2, x_1 = mole fraction of species 1,

x_2 is the mole fraction of species 2, v_i is the velocity of species 1, v_j is the velocity of species 2, $\bar{v}_i$ is the average velocity of species 1, and $\bar{v}_j$ is the average velocity of species 2 (Sharma, et al., 2011; Zhou, et al., 2005; Zhou, et al., 1996):

$$D_{12} = \left(\frac{1}{N x_1 x_2}\right)\left[\frac{1}{3}\int_0^{\infty} \langle \dot{A}(t)\dot{A}(0)\rangle dt\right] \tag{30}$$

$$\dot{A}(t) = x_2 \sum_{i=1}^{N_1} v_i(t) - x_1 \sum_{j=1}^{N_2} v_j(t) = N x_1 x_2 \left(\bar{v}_i(t) - \bar{v}_j(t)\right) \tag{31}$$

Using Equations (28) and (30), the one dimensional (d = 1) mutual diffusion coefficient can be estimated using mean-square displacement as follows, where z_i is the z coordinate of species 1, z_j is the z coordinate of species 2, $\bar{z}_i$ is the average z coordinate species 1, $\bar{z}_j$ is the average z coordinate species 2:

$$D_{12} = \left(\frac{1}{N x_1 x_2}\right)\left[\frac{\langle [A(t) - A(0)]^2\rangle}{2t}\right] = N x_1 x_2 \frac{MSD_{collective}}{2t} \tag{32}$$

$$A(t) = x_2 \sum_{i=1}^{N_1} z_i(t) - x_1 \sum_{j=1}^{N_2} z_j(t) = N x_1 x_2 \left[\bar{z}_i(t) - \bar{z}_j(t)\right] \tag{33}$$

$$MSD_{collective} = \left\langle \left[\left[\bar{z}_i(t) - \bar{z}_j(t) \right] - \left[\bar{z}_i(0) - \bar{z}_j(0) \right] \right]^2 \right\rangle \qquad (34)$$

The average coordinates ($\bar{z}_i \; and \; \bar{z}_j$) can be estimated from MD simulation trajectories and so Equations (32), (33), and (34) can be used to estimate self (for $i = j$) and mutual (for $i \neq j$) diffusion coefficients and these values can be compared to results from other theories.

Estimating Diffusion Coefficients

The example VMD scripts shown in **Table H - 1** and **Table H - 2** (Appendix H: Example VMD Script Files for Trajectory Analysis) are used to estimate single particle and collective mean-square displacement (MSD), respectively.

The MSD was defined as a time average in Equation (28). For a given time delay t, the $MSD_{single-particle}$ can be estimated using Equation (35), and the $MSD_{collective}$ can be estimated using Equation (36), where M is the number of available time origins and N is the number of molecules (Haile, 1992; Leach, 2001):

$$MSD_{single-particle}(t) = \frac{1}{M * N} \sum_{M} \sum_{N} [A(t) - A(0)]^2 \qquad (35)$$

$$MSD_{collective}(t) = \frac{1}{M}\sum_{M}[A(t) - A(0)]^2 \quad (36)$$

The scripts in **Table H - 1** and **Table H - 2** estimate the MSD at various time delays and save this information to an output file. This data is then imported into Microsoft Excel and Equations (37) and (38), are used to estimate self and mutual diffusion coefficients, respectively.

$$D_{self} = \frac{1}{6} * \frac{d(MSD_{single-particle})}{dt} \quad (37)$$

$$D_{12} = \frac{Nx_1x_2}{2} * \frac{d(MSD_{collective})}{dt} \quad (38)$$

3.4.6.2 Relative Solvent Drying Times

Relative solvent drying times can also be estimated from MD simulations. Solvent evaporation rates have been measured and published as the ratio of drying times; these ratios are reported relative to a reference solvent (Wilson, 1955).

The ratio of drying times can be expressed as follows, where t_i is the evaporation time for a drop of solvent i, t_{ref} is the evaporation time for a drop of the reference solvent, V is the volume of solvent drop (constant for all solvents), ρ_i is the

density of solvent i, ρ_{ref} is the density of the reference solvent, v_i is the center of mass (COM) velocity of solvent i, v_{ref} is the COM velocity of the reference solvent, N_i is the evaporative flux of solvent i, N_{ref} is the evaporative flux of the reference solvent, A_i is the evaporation area for solvent i, A_{ref} is the evaporation area for the reference solvent:

$$\frac{t_i}{t_{ref}} = \frac{{\rho_i V}/{N_i A_i}}{{\rho_{ref} V}/{N_{ref} A_{ref}}} = \frac{{\rho_i V}/{\rho_i v_i A_i}}{{\rho_{ref} V}/{\rho_{ref} v_{ref} A_{ref}}} = \frac{v_{ref} A_{ref}}{v_i A_i} \qquad (39)$$

The center of mass (COM) velocities ($v_i \; and \; v_{ref}$) and the evaporation areas ($A_i \; and \; A_{ref}$) can be estimated from MD simulation trajectories and so Equation (39) can be used to estimate relative evaporation rates and these values can be compared to published values.

Estimating Relative Evaporation Rates

An illustration of how MD simulation can be used to estimate liquid evaporation is shown in **Figure 8**. The example VMD script file shown in **Table H - 3** (Appendix H: Example VMD Script Files for Trajectory Analysis) is used to track the spread of liquid Acetone into Air by tabulating various center of mass (COM) locations; the initial configuration for this system is illustrated in **Figure 17**. The VMD

script writes this data to an output file which is then imported into Microsoft Excel. The data is then analyzed to estimate the rate of liquid spread, which can be used to estimate the COM velocities in Equation (39) and then relative solvent drying times can be estimated and compared to reported values.

Figure 8: Using MD simulation to estimate liquid evaporation rates.

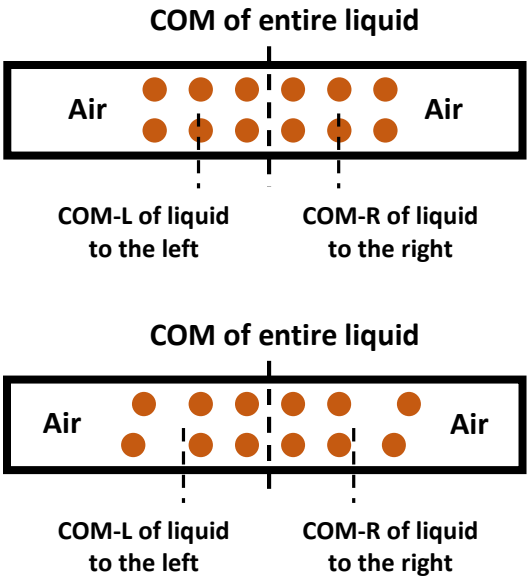

Starting configuration (t=0); liquid layer sandwiched between Air; Periodic Boundary Conditions (PBCs) used in all directions, the air space is much larger in length than thickness of liquid layer.

As the liquid evaporates it will spread, which should show in the COM to COM-L/R distance. The rate of this spread can be used to estimate the velocity of the liquid and thus the evaporation rate.

3.5 Results and Discussion

In this work, two basic types of simulations have been performed. One type is used to estimate diffusion coefficients and results are compared with Chapman-Enskog (CE) theory (see Appendix I: Chapman-Enskog Theory). The other type is used to estimate the relative solvent drying times of liquids in Air and results are compared

with experimentally measured values (Wilson, 1955). Simulation results are presented in this chapter along with discussion.

3.5.1.1 Diffusion Coefficients

A typical starting configuration for an MD simulation used to estimate diffusion coefficients is illustrated in **Figure 9**. In this work, self and mutual diffusion coefficients are estimated from the mean-square displacement (MSD). Self-diffusion coefficients are estimated using both, the single-particle and collective MSD, while mutual diffusion coefficients are estimated using the collective MSD. Estimates based on MD simulation are compared to those from Chapman-Enskog (CE) theory.

For the case of estimating self-diffusion from the single-particle MSD, the filled and unfilled circles in **Figure 9** represent the same molecule. For the case of estimating self-diffusion from the collective MSD, the filled and unfilled circles represent the same molecule but they are tagged as “filled” or “unfilled”. Lastly, for the case of estimating mutual diffusion from the collective MSD, the filled and unfilled circles represent different molecules.

Figure 9: Illustration of a typical starting configuration for an MD simulation used to estimate self and mutual diffusion coefficients.

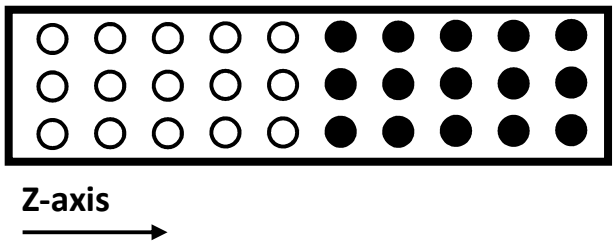

Self-Diffusion Coefficients

Self-diffusion coefficients were estimated for the chemicals listed in **Table 7** using both, single-particle and collective MSD. All simulations were run at 400 K, the number of molecules in the simulation cell was 200, and simulation were run for 2 ns. The density and temperature correspond approximately to a pressure of 1 atm (see Appendix K: Material Properties for MD Simulations).

Table 7: MD simulation was used to estimate self-diffusion coefficients for the following chemicals; the simulation temperature, number of molecules (N), and simulation box dimensions are also listed; the density and temperature correspond approximately to a pressure of 1 atm; simulations were run for 2 ns.

Chemical	Simulation Temperature in Kelvin (K)	Number of molecules (N)	Simulation Box Dimensions (X, Y, Z) in Angstroms (Å)
Acetone	400	200	(100, 100, 1096)
Carbon Dioxide	400	200	(100, 100, 1104)
Methane	400	200	(100, 100, 1106)
Propane	400	200	(100, 100, 1100)
Water	400	200	(100, 100, 1094)

The single particle and collective MSD for the five gases listed in **Table 7** are shown in **Figure 10** and **Figure 11**, respectively. Self-diffusion coefficients estimated using MD simulation (single particle and collective MSD) are compared with Chapman-Enskog (CE) values in **Figure 12** (bar chart) and **Figure 13** (scatter chart).

Figure 10: Single particle mean square displacement (MSD) for various gasses at atmospheric pressure; time delay of 0.2 ns to 1.8 ns was used to estimate the slope of MSD vs time delay.

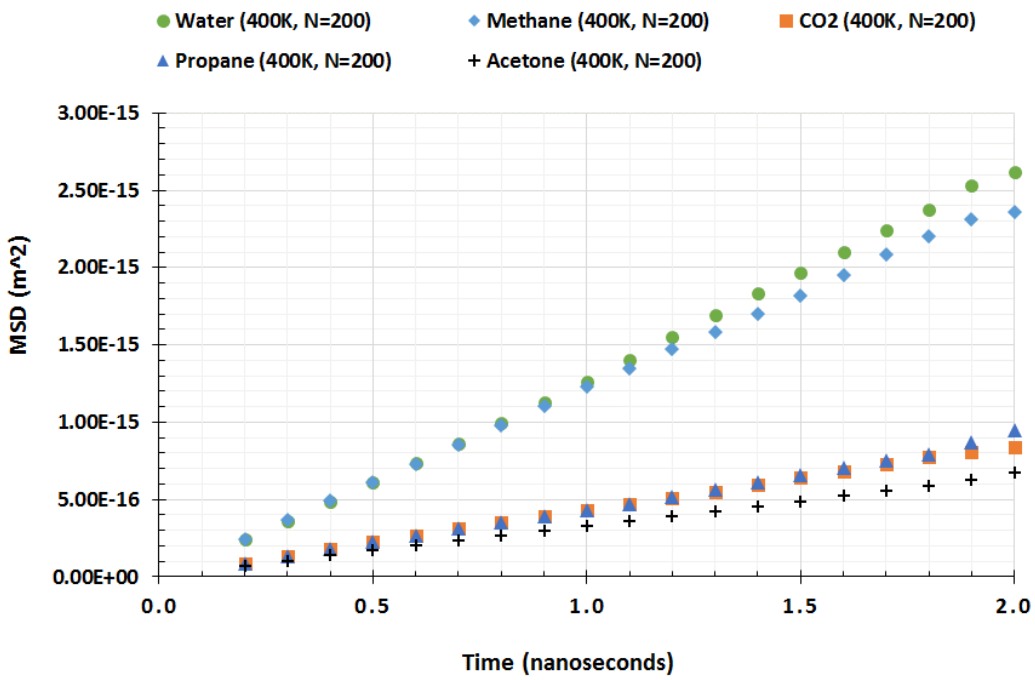

Figure 11: Collective mean square displacement (MSD) for "tagged" equimolar binary gas mixtures at atmospheric pressure; time delay of 0.5 ns to 1.5 ns was used to estimate the slope of MSD vs time delay.

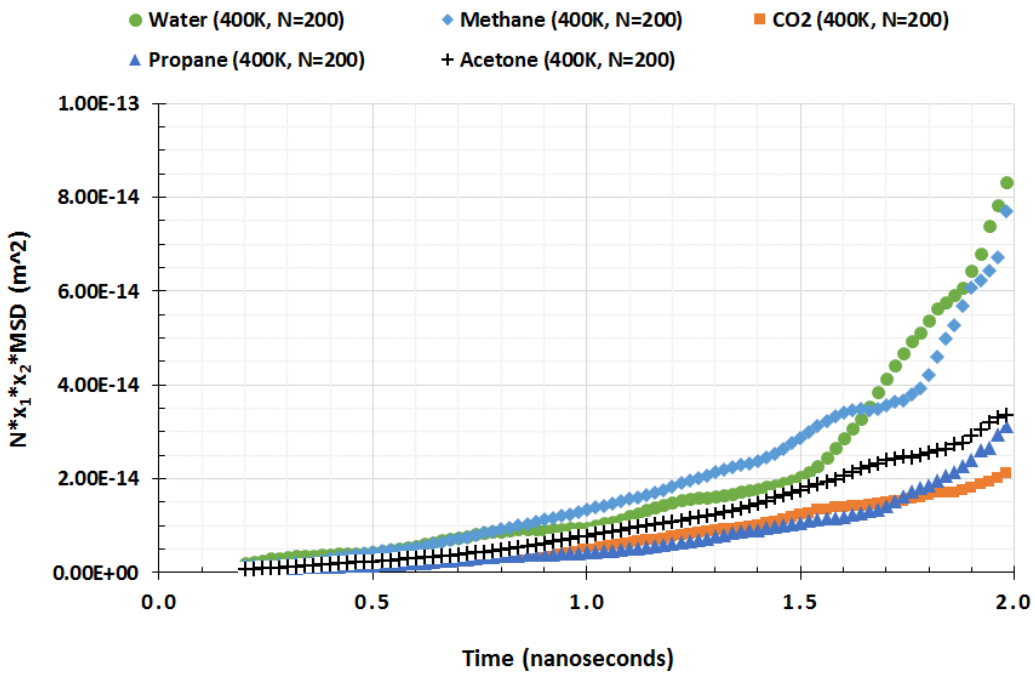

Figure 12: Bar chart; self-diffusion coefficients for various gases at atmospheric pressure; estimates from single particle and collective MSD are compared with Chapman-Enskog.

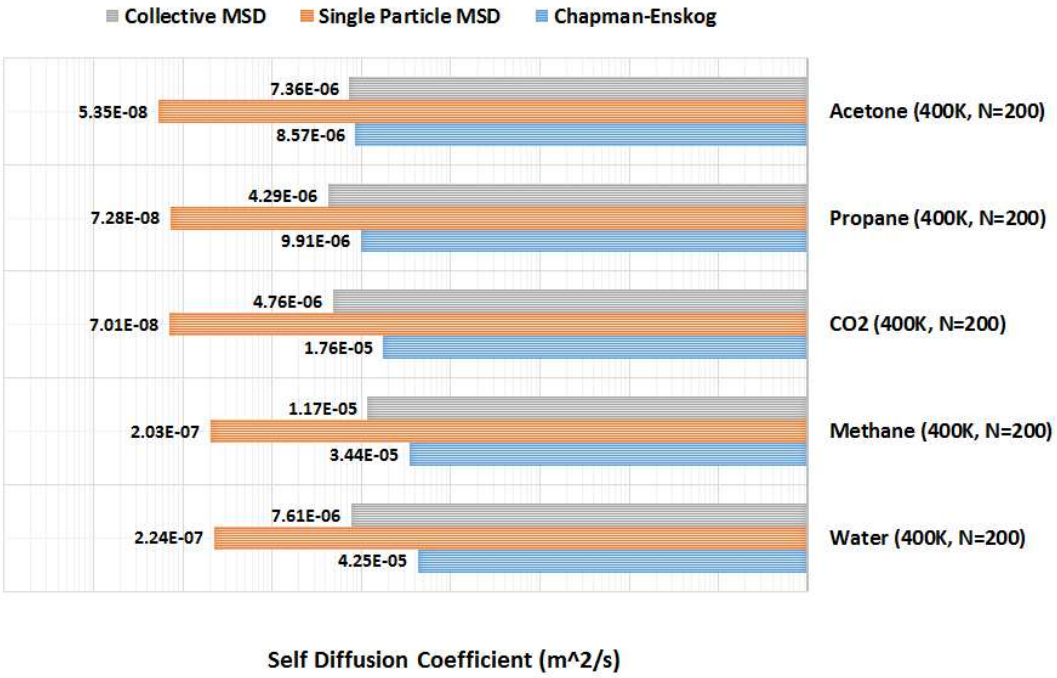

Figure 13: Scatter chart; self-diffusion coefficients for various gases at atmospheric pressure; estimates from single particle and collective MSD are compared with Chapman-Enskog.

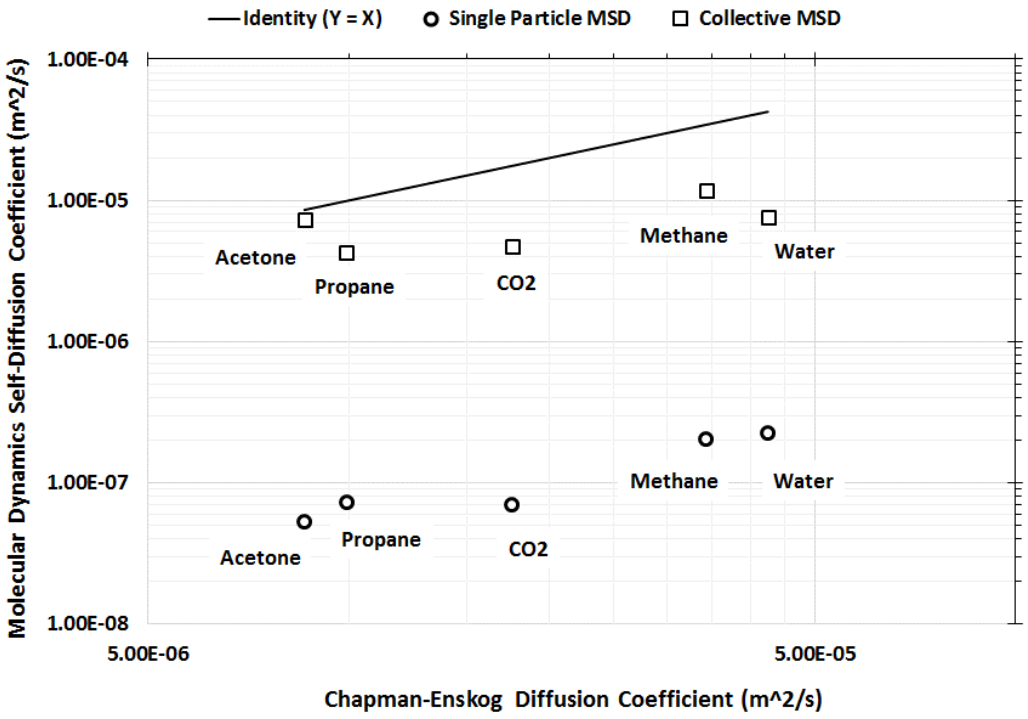

Mutual Diffusion Coefficients

Mutual diffusion coefficients were estimated for the binary gas mixtures listed in **Table 8** using collective MSD. All simulations were for equimolar binary gas mixtures and 2 ns in duration. The density and temperature correspond approximately to a pressure of 1 atm (see Appendix K: Material Properties for MD Simulations).

Table 8: MD simulation was used to estimate mutual-diffusion coefficients for the following equimolar binary gas mixtures; the simulation temperature, number of molecules (N) of each mixture component, and simulation box dimensions are also listed; the density and temperature correspond approximately to a pressure of 1 atm; simulations were run for 2 ns.

Binary Gas Mixture	**Simulation Temperature in Kelvin (K)**	**Number of molecules (N)**	**Simulation Box Dimensions (X, Y, Z) in Angstroms (Å)**
Propane/Carbon Dioxide	298	266	(100, 100, 1100)
Water/Methane	400	200	(100, 100, 1100)
Water/Carbon Dioxide	400	200	(100, 100, 1100)
Methane/Carbon Dioxide	298	266	(100, 100, 1093)
Acetone/Propane	400	200	(100, 100, 1098)
Acetone/Water	400	200	(100, 100, 1096)

The collective MSD for the six equimolar binary gas mixtures listed in **Table 8** is shown in **Figure 14**. Mutual diffusion coefficients estimated using MD simulation are compared with Chapman-Enskog (CE) values in **Figure 15** (bar chart) and **Figure 16** (scatter chart).

Figure 14: Collective mean square displacement (MSD) for equimolar binary gas mixtures at atmospheric pressure; time delay of 0.6 ns to 1.6 ns was used to estimate the slope of MSD vs time delay.

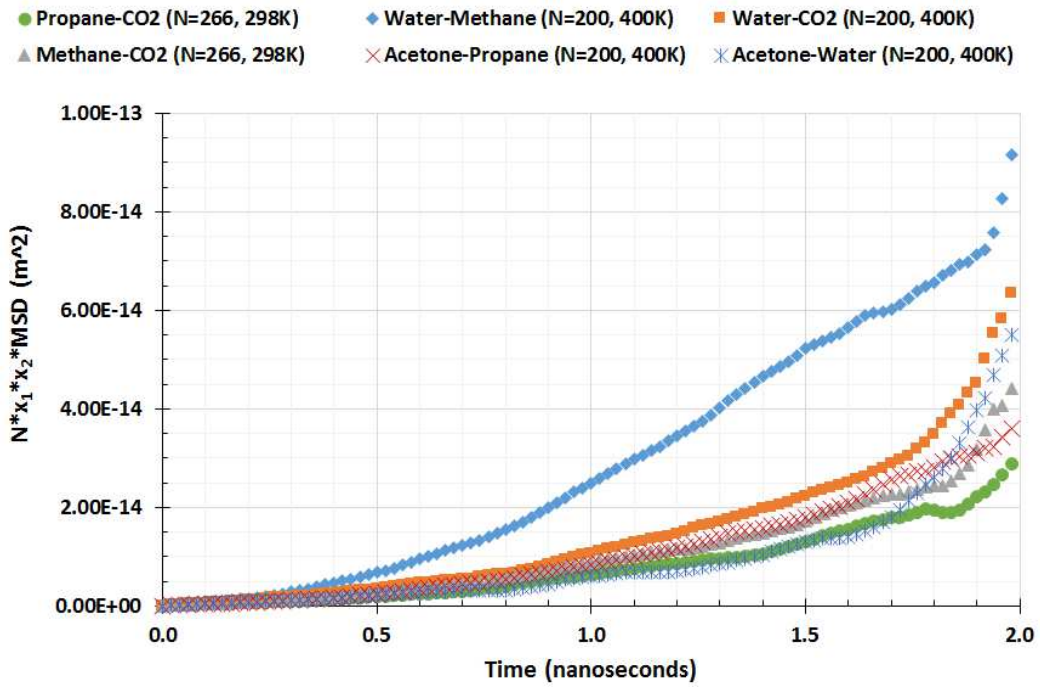

Figure 15: Bar chart; binary gas diffusion coefficients at atmospheric pressure; Molecular Dynamics (MD) vs Chapman-Enskog (CE) Theory.

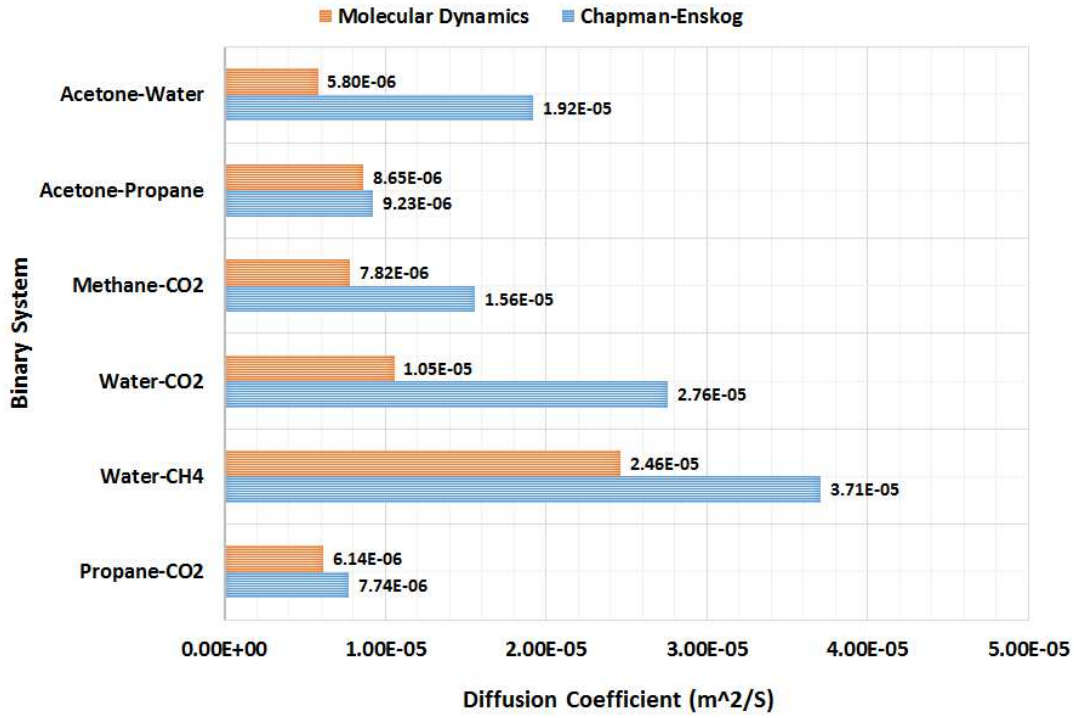

Figure 16: Scatter chart; binary gas diffusion coefficients at atmospheric pressure; Molecular Dynamics (MD) vs Chapman-Enskog (CE) Theory.

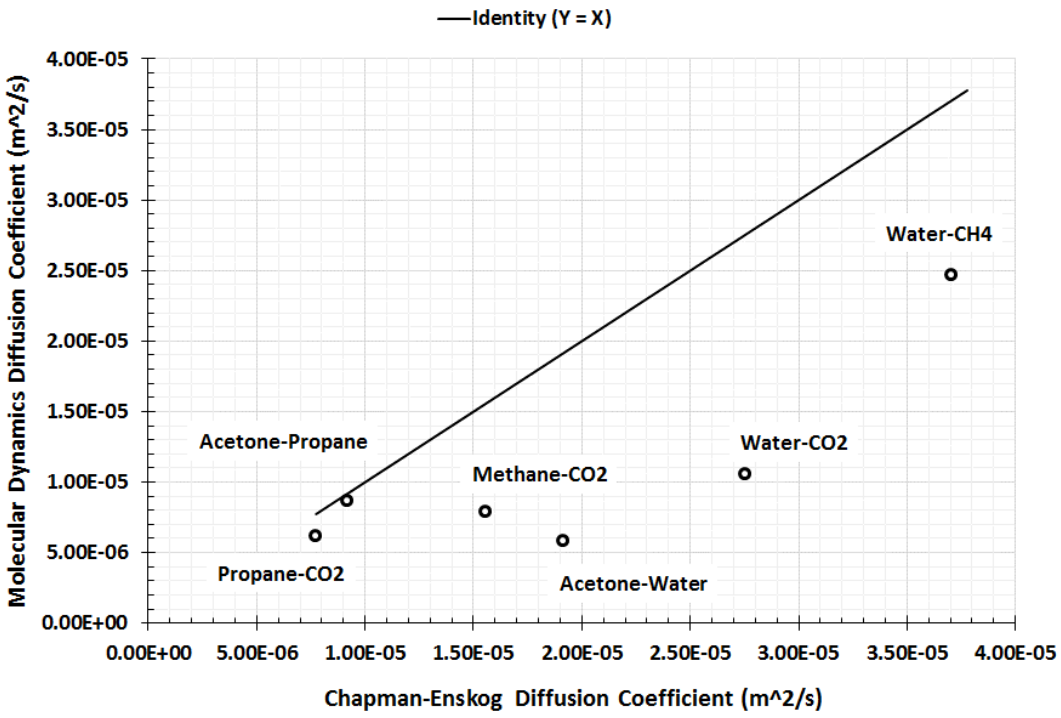

This work was driven by a simple question. If MD simulation is used to estimate diffusion coefficients, how will these estimates compare to results from Chapman-Enskog theory?

The single particle MSD is often used to characterize the mobility or self-diffusion coefficient of molecules. However, one important observation from this work is that single particle MSD does not yield good estimates of mobility or self-diffusion coefficients for gases for simulations that are 2 ns in duration. When compared to CE values, MD estimates for self-diffusion using single particle MSD are approximately

an order of magnitude too small; relative to CE, these values exhibit an average absolute deviation (AAD) of 99%.

When the collective MSD is used to estimate self and mutual diffusion coefficients with simulations runs of 2 ns, MD estimates are similar in magnitude to CE values and exhibit an AAD of 58% (self-diffusion) and 40% (mutual diffusion).

Although using collective MSD leads to better estimates, MD simulations systematically under predict compared to CE theory. This suggests that the TraPPE and TIP3P potentials used in this work are not optimized for estimating gas phase transport properties such as diffusion coefficients. For example, TraPPE potentials were optimized using phase equilibria data.

Single particle and collective MSD are expected to yield similar values for diffusion coefficients. The two approaches differ in their simulation methodology. The single particle method uses unwrapped trajectories to estimate MSD while the collective method uses PBCs in all Cartesian directions and estimates MSD based on the COM distance between the two diffusing gases. It may be that one method requires much longer simulation times. For example, when simulating dilute gases using OPLS-AA potential parameters, simulation times of 14 ns were used to estimate diffusion coefficients (Chae, et al., 2011). However, when simulating liquid systems using TraPPE potential parameters, simulation times of 30 ns were used to estimate diffusion coefficients (Makrodimitri, et al., 2011). For this work, simulation times of up to 20 ns for water vapor were investigated but no difference was observed in the single

particle MSD when compared to a 2 ns run. Simulations of methane gas with up to 10,000 molecules were also investigated but no difference was observed in the single particle MSD when compared to a system with 200 methane molecules.

This work starts to quantify the accuracy one can expect when estimating transport properties such as diffusion coefficients using potentials that have been parameterized using phase equilibria data. Based on the results of this work, collective MSD simulations of about 2 ns should yield results to within an order of magnitude.

In addition, observations from this work also highlight an opportunity for developing potentials parameterized using transport data and then comparing the performance of these potentials when they are used to estimate phase equilibria.

3.5.1.2 Relative Solvent Drying Times

A typical starting configuration for an MD simulation used to estimate relative solvent drying times is illustrated in **Figure 17**. A thin layer of liquid (filled circles) is sandwiched between layers of Air (unfilled circles). The thickness of the liquid layer is much smaller than the length of the simulation box in the Z direction. As liquid evaporates, it spreads and the rate of this spread can be used to estimate relative evaporation rates (see Chapters 3.4.6.2 and 3.4.6). These types of evaporation rates are reported relative to a reference material. In this work, the reference material is Diethyl Ether; experimentally measured values are also reported relative to this material (Wilson, 1955).

Figure 17: Illustration of a typical starting configuration for an MD simulation used to estimate relative solvent drying times of liquids in Air.

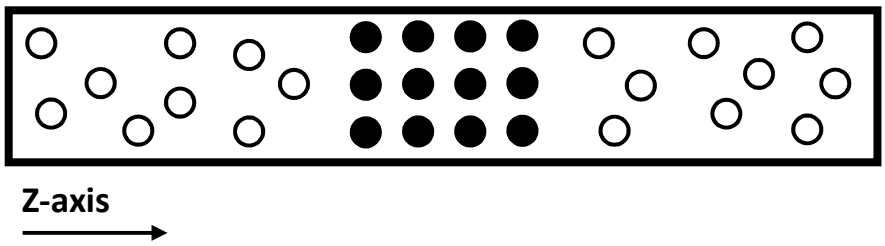

Relative solvent drying times were estimated for the chemicals listed in **Table 9**. All simulations were run at 296 K. The number of molecules (N) is specified as N_1/N_2, where N_1 is the number of molecules of the evaporating chemical and N_2 is the number of Air molecules; Air is comprised of Nitrogen (79%) and Oxygen (21%) molecules. The density and temperature correspond approximately to a pressure of 1 atm (see Appendix K: Material Properties for MD Simulations).

Table 9: MD simulation was used to estimate relative solvent drying times for the following chemicals; the simulation temperature, number of molecules of the evaporating chemical (N_1), number of Air molecules (N_2), and simulation box dimensions are also listed; the density and temperature correspond approximately to a pressure of 1 atm.

Chemical	Simulation Temperature in Kelvin (K)	Number of molecules (N_1/N_2)	Simulation Box Dimensions (X, Y, Z) in Angstroms (Å)
Acetone	296	400/200	(30, 30, 9724)
Benzene	296	400/200	(32, 32, 8542)
Cyclohexane	296	400/200	(34, 34, 7508)
Diethyl Ether	296	400/200	(33, 33, 7734)
Ethanol	296	800/200	(35, 35, 7164)
Methanol	296	800/200	(31, 31, 9078)
n-Pentane	296	400/200	(35, 35, 7188)
2-Pentanone	296	400/200	(34, 34, 7614)

As liquid evaporates it will spread, which should show in the COM to COM-L/R distance (see **Figure 8**). This spread is summarized in **Table 10** and also characterized in **Figure J - 1** to **Figure J - 8** for the chemicals listed in **Table 9** (see Appendix J: Rate of Spread). Relative solvent drying times using MD simulation are compared with experimentally measured values in **Figure 18** (bar chart) and **Figure 19** (scatter chart). In addition, the SM2E model is also used to estimate relative solvent drying times for an isothermal case and a non-isothermal case in which evaporative cooling is taken into account.

Table 10: Average rate of solvent spread during liquid evaporation as measured from MD simulation; see **Figure 8** for an illustration; relative solvent drying times are estimated based on the average rate of spread as shown in Equation (39).

Chemical	Rate of Spread (cm/s)	
	Left Side	Right Side
Acetone	5.542	4.367
Benzene	2.358	0.770
Cyclohexane	0.197	0.192
Diethyl Ether	8.356	4.809
Ethanol	0.521	0.464
Methanol	0.644	0.249
n-Pentane	7.569	9.964
2-Pentanone	0.006	0.015

Figure 18: Bar chart; relative solvent drying times at 296 K and 1 atm; MD simulation estimates are compared with experimentally measured values.

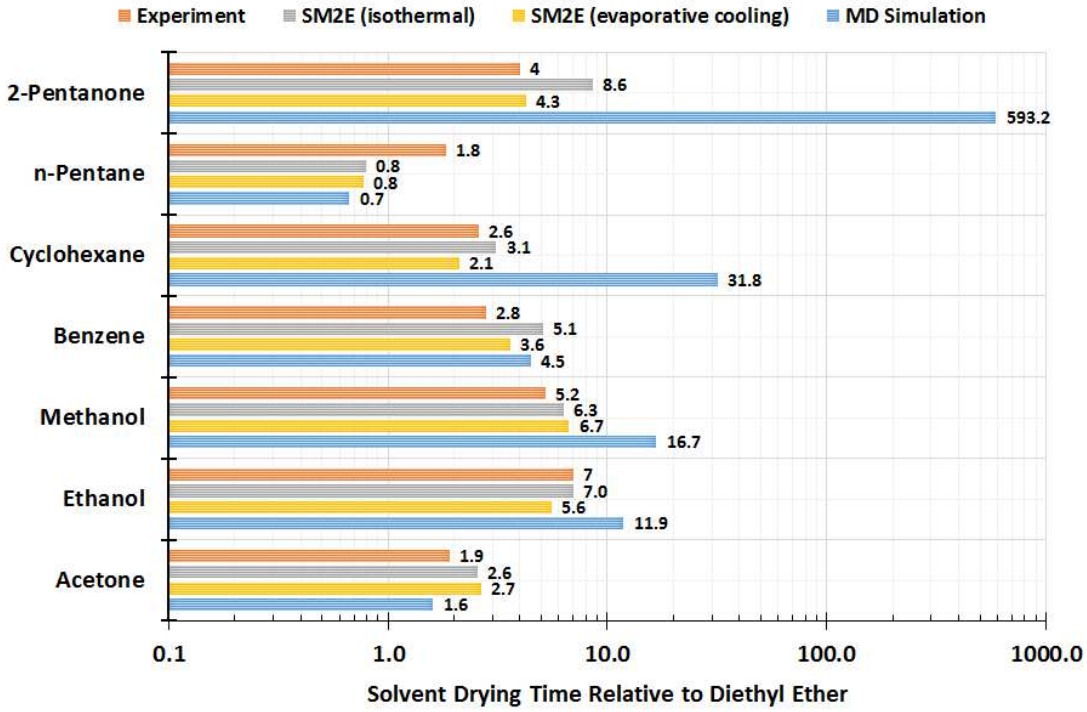

Figure 19: Scatter chart; relative solvent drying times at 296 K and 1 atm; MD simulation estimates are compared with experimentally measured values

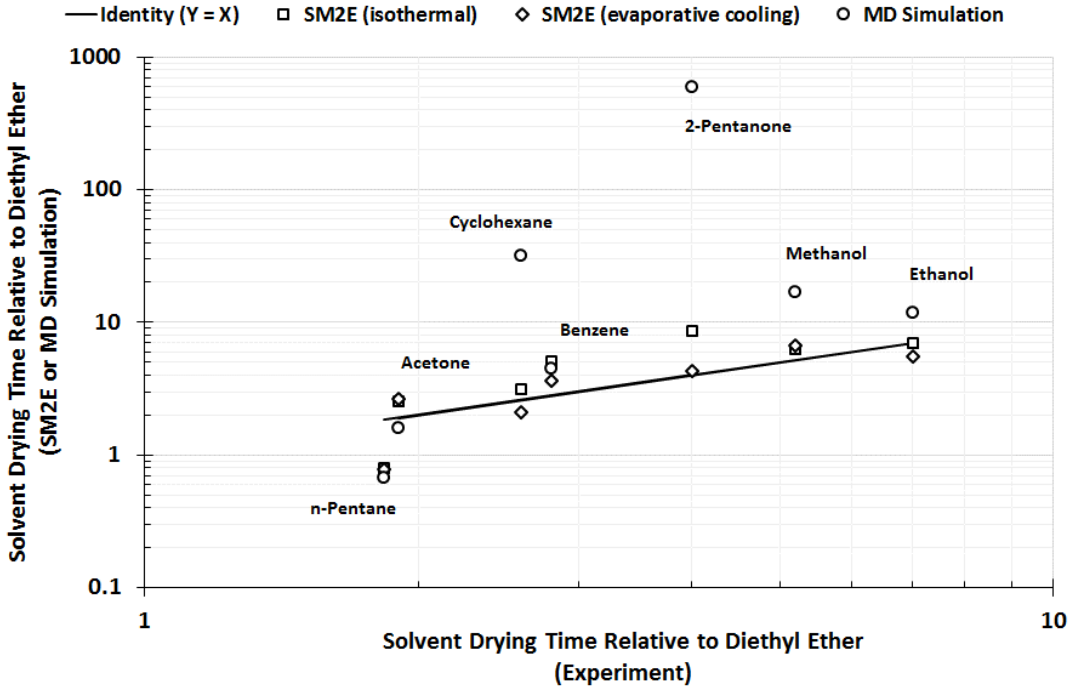

This work was driven by a simple question. If MD simulation is used to estimate relative solvent drying times of liquids into Air, how will these estimates compare to experimentally measured values or modeled values?

One important observation from this work is that even for the relatively small systems simulated in this work, in most cases, simulation times of 10 to 20 nanoseconds (ns) are needed to adequately characterize the spread of the evaporating liquid.

In most cases, results from MD simulation are within an order of magnitude of measured values. The notable exceptions are Cyclohexane and 2-Pentanone. This observation is interesting because Benzene and Cyclohexane are both cyclic compounds, while Acetone and 2-Pentanone are both Ketones. But the dynamics of Cyclohexane and 2-Pentanone are observed to be much slower than Benzene and Acetone, respectively (see **Table 10**); suggesting TraPPE intermolecular attractions may be too strong.

Since the TraPPE potentials used in this work are optimized using phase equilibria data, they may not be adequate for estimating transport properties such as relative solvent drying times in all cases. This work starts to quantify the accuracy one can expect when estimating transport properties such as relative evaporation rates from potentials that have been parameterized using phase equilibria data.

Using the SM2E model yields more consistent results and does not require as much computational effort. So why even explore MD simulation for estimating these properties? Well, although it may be more practical to use the SM2E model for estimation purposes, this work highlights an opportunity for developing potentials that are parameterized using transport data and then assessing the performance of these potentials when they are used to estimate equilibrium properties. Such potentials may be better candidates for studying the dynamics of a system.

Appendix A: Example MDL Molfile Coordinate File (Methane)

The contents of an MDL Molfile for Methane are included in **Table A - 1**. The first three lines constitute a header section. Line 1 specifies the molecule's name, which is "297" in this case. Line 2 says that the molecule was generated by "Marvin 12300703363D". Line 3 is a comment line and in this case it is blank.

Line 4 is referred to as the "counts" line and identifies the number of atoms and bonds in the molecule; 5 atoms and 4 bonds in this case. Lines 5-9 is the "Atom block" and describes each atom's Cartesian coordinates (x, y, z) in angstroms and the atomic symbol.

Lines 10-13 is the "Bonds block" and each line describes a bond. For example, Line 10 identifies the atoms in the bond (atoms 1 and 2), and the bond type (bond type "1" means single bond). Line 14 is the termination line.

Table A - 1: Contents of a Methane MDL Molfile obtained from ChemSpider.

1.	297
2.	Marvin 12300703363D
3.	
4.	5 4 0 0 0 0 999 V2000
5.	-0.0000 -0.0000 0.0000 C 0 0 0 0 0 0 0 0 0 0 0 0
6.	1.0900 -0.0000 0.0000 H 0 0 0 0 0 0 0 0 0 0 0 0
7.	-0.3633 1.0277 0.0000 H 0 0 0 0 0 0 0 0 0 0 0 0
8.	-0.3633 -0.5138 0.8900 H 0 0 0 0 0 0 0 0 0 0 0 0
9.	-0.3633 -0.5138 -0.8900 H 0 0 0 0 0 0 0 0 0 0 0 0
10.	1 2 1 0 0 0 0
11.	1 3 1 0 0 0 0
12.	1 4 1 0 0 0 0
13.	1 5 1 0 0 0 0
14.	M END

Appendix B: Example PDB Coordinate File (Methane)

The contents of a PDB file for Methane are included in **Table B - 1**. Each line represents a particular type of record. For example, REMARK records can contain free-form explanations or comments; HETATM records list Cartesian coordinates (x, y, z) in angstroms for hetero-atoms, atoms that are not part of a protein molecule; CONECT records describe connectivity between atoms; and the END record marks the end of the PDB file.

Table B - 1: Contents of a Methane PDB file obtained from Open Babel.

REMARK 1 2 3 4 5 6 7 8
REMARK78901234567890123456789012345678901234567890123456789012345678901234567890
COMPND 297
AUTHOR GENERATED BY OPEN BABEL 2.3.2
HETATM 1 C1 MET 1 0.000 0.000 0.000 1.00 0.00 C
HETATM 2 H1 MET 1 1.090 0.000 0.000 1.00 0.00 H
HETATM 3 H2 MET 1 -0.363 1.028 0.000 1.00 0.00 H
HETATM 4 H3 MET 1 -0.363 -0.514 0.890 1.00 0.00 H
HETATM 5 H4 MET 1 -0.363 -0.514 -0.890 1.00 0.00 H
CONECT 1 2 3 4 5
CONECT 1
CONECT 2 1
CONECT 3 1
CONECT 4 1
CONECT 5 1
MASTER 0 0 0 0 0 0 0 0 5 0 5 0
END

Appendix C: Example PACKMOL Configuration Files

The PACKMOL input file used to prepare an initial configuration for estimating diffusion for a gas mixture of Methane and Carbon Dioxide at approximately 298 K and 1 atm is included in **Table C - 1**. This input file defines a rectangular box whose dimensions are specified in Angstroms. Methane molecules are placed on one side of the box and Carbon Dioxide molecules on the other side, creating a concentration gradient along the Z axis.

Table C - 1: PACKMOL input file for estimating diffusion for a Methane-Carbon Dioxide gas mixture at approximately 298 K and 1 atm; all dimensions are in Angstroms.

```
# Methane-CO2 Mixture at 298 K and 1 atm

# All the atoms from different molecules will be separated at least 2.0
# Angstroms at the solution.
tolerance 2.0

# The file type of input and output files is PDB
filetype pdb

# Increase maximum system dimensions
sidemax 5000.d0

# The name of the output file
output mixture.pdb

# Place molecules inside a box
structure methane.pdb
  number 133
  inside box 0.0 0.0 0.0 100.0 100.0 547.0
end structure

structure carbon_dioxide.pdb
  number 133
  inside box 0.0 0.0 -546.0 100.0 100. 0.0
end structure
```

The PACKMOL input file used to prepare an initial configuration for estimating evaporation of a liquid layer of Acetone sandwiched between Air at approximately 296 K and 1 atm is included in **Table C - 2**.

Table C - 2: PACKMOL input file for estimating evaporation of an Acetone-Air system at approximately 296 K and 1 atm; all dimensions are in Angstroms.

```
# Acetone-Air Mixture at 296 K and 1 atm

# All the atoms from different molecules will be separated at least 2.0
# Angstroms at the solution.
tolerance 2.0

# The file type of input and output files is PDB
filetype pdb

# Increase maximum system dimensions
sidemax 9999.d0

# The name of the output file
output mixture.pdb

# Place molecules inside a box
structure acetone.pdb
  number 400
  inside box 0.0 0.0 4832.0 30.0 30.0 4892.0
end structure

structure nitrogen.pdb
  number 79
  inside box 0.0 0.0 0.0 30.0 30.0 4832.0
end structure

structure oxygen.pdb
  number 21
  inside box 0.0 0.0 0.0 30.0 30.0 4832.0
end structure

structure nitrogen.pdb
  number 79
  inside box 0.0 0.0 4892.0 30.0 30.0 9724.0
end structure

structure oxygen.pdb
  number 21
  inside box 0.0 0.0 4892.0 30.0 30.0 9724.0
end structure
```

Appendix D: NAMD Topology File

Table D - 1: NAMD topology file used for MD simulations.

```
!          Atom Type
MASS     1 CH4          16.04300 C ! CH4 pseudo atom, UA traPPE Alkanes
MASS     2 CH3          15.03500 C ! CH3 pseudo atom, UA traPPE Alkanes
MASS     3 CH2          14.02700 C ! CH2 pseudo atom, UA traPPE Alkanes
MASS     4 CH           13.01900 C ! CH psuedo atom, UA traPPE Alkanes
MASS     5 C            12.01100 C ! C pseudo atom, UA traPPE Alkanes
MASS     6 OT           15.99940 O ! TIPS3P WATER OXYGEN
MASS     7 HT           1.00800  H ! TIPS3P WATER HYDROGEN
MASS     8 CS           12.01100 C ! C pseudo atom, traPPE-small CO2
MASS     9 OS           15.99940 O ! O pseudo atom, traPPE-small CO2
MASS    10 CK           12.01100 C ! C pseudo atom, UA traPPE ketone
MASS    11 C3K          15.03500 C ! CH3 pseudo atom, UA traPPE ketone
MASS    12 OK           15.99940 O ! O pseudo atom, UA traPPE ketone
MASS    13 O2           10.66627 O ! O pseudo atom, traPPE-small O2
MASS    14 MO2          10.66627 M ! M (dummy) pseudo atom, traPPE-small O2
MASS    15 N2           9.33800  N ! N pseudo atom, traPPE-small N2
MASS    16 ZO2          9.33800  Z ! Z (dummy) pseudo atom, traPPE-small N2
MASS    17 EH3          15.03500 C ! CH3 pseudo atom, UA traPPE Ethers
MASS    18 EH2          14.02700 C ! CH2 pseudo atom, UA traPPE Ethers
MASS    19 EO           15.99940 O ! O pseudo atom, UA traPPE Ethers
MASS    20 AO           15.99940 O ! O pseudo atom, UA traPPE Alcohols
MASS    21 HA           1.00800  H ! H pseudo atom, UA traPPE Alcohols
MASS    22 CC2          14.02700 C ! CH2 pseudo atom, UA traPPE Cyclic Alkanes
MASS    23 C2K          14.02700 C ! CH2 pseudo atom, UA traPPE ketone
MASS    24 ACH          13.01900 C ! CH psuedo atom, UA traPPE Aromatics


DEFA FIRS NONE LAST NONE
AUTO ANGLES DIHE

RESI    MET         0.000 ! Methane molecule
GROUP
ATOM C1    CH4   0.000
PATCHING FIRS NONE LAST NONE

RESI ETH         0.000 ! Ethane molecule
GROUP
ATOM C1    CH3    0.000
ATOM C2    CH3    0.000
BOND C1 C2
PATCHING FIRS NONE LAST NONE

RESI PRO          0.000 ! Propane molecule
GROUP
ATOM C1    CH2    0.000
ATOM C2    CH3    0.000
ATOM C3    CH3    0.000
BOND C1 C2 C1 C3
PATCHING FIRS NONE LAST NONE

RESI MOH          0.000 ! Methanol molecule
GROUP
ATOM C1    CH3    0.265
ATOM O1    AO    -0.700
```

```
ATOM H1    HA     0.435
BOND C1 O1 O1 H1
PATCHING FIRS NONE LAST NONE

RESI EOH          0.000 ! Ethanol molecule
GROUP
ATOM C3    CH3    0.000
ATOM C2    CH2    0.265
ATOM O1    AO    -0.700
ATOM H1    HA     0.435
BOND C3 C2 C2 O1 O1 H1
PATCHING FIRS NONE LAST NONE

RESI BUT          0.000 ! n-butane molecule
GROUP
ATOM C1     CH3     0.000
ATOM C2     CH2     0.000
ATOM C3     CH2     0.000
ATOM C4     CH3     0.000
BOND C1 C2 C2 C3 C3 C4
PATCHING FIRS NONE LAST NONE

RESI PEN          0.000 ! n-Pentane molecule
GROUP
ATOM C1     CH2     0.000
ATOM C2     CH2     0.000
ATOM C3     CH2     0.000
ATOM C4     CH3     0.000
ATOM C5     CH3     0.000
BOND C1 C2 C1 C3 C2 C4 C3 C5
PATCHING FIRS NONE LAST NONE

RESI CHX          0.000 ! Cyclohexane molecule
GROUP
ATOM C1     CC2     0.000
ATOM C2     CC2     0.000
ATOM C3     CC2     0.000
ATOM C4     CC2     0.000
ATOM C5     CC2     0.000
ATOM C6     CC2     0.000
BOND C1 C2 C1 C3 C2 C4 C3 C5 C4 C6 C5 C6
PATCHING FIRS NONE LAST NONE

RESI BNZ          0.000 ! Benzene molecule
GROUP
ATOM C1     ACH     0.000
ATOM C2     ACH     0.000
ATOM C3     ACH     0.000
ATOM C4     ACH     0.000
ATOM C5     ACH     0.000
ATOM C6     ACH     0.000
BOND C1 C3 C2 C4 C5 C6
DOUBLE C1 C2 C3 C5 C4 C6
PATCHING FIRS NONE LAST NONE

RESI DEE          0.000 ! Diethyl Ether molecule
GROUP
ATOM O1     EO     -0.500
ATOM C1     EH2     0.250
ATOM C2     EH2     0.250
ATOM C3     EH3     0.000
```

```
ATOM C4     EH3     0.000
BOND O1 C1 O1 C2 C1 C3 C2 C4
PATCHING FIRS NONE LAST NONE

RESI CO2         0.000 ! Carbon Dioxide molecule
GROUP
ATOM C1    CS    0.700
ATOM O1    OS   -0.350
ATOM O2    OS   -0.350
BOND C1 O1 C1 O2
PATCHING FIRS NONE LAST NONE

RESI ACE         0.000 ! Acetone molecule
GROUP
ATOM O1    OK   -0.424
ATOM C1    CK    0.424
ATOM C2    C3K   0.000
ATOM C3    C3K   0.000
BOND C1 C2 C1 C3
DOUBLE C1 O1
PATCHING FIRS NONE LAST NONE

RESI 2PN         0.000 ! 2-Pentanone molecule
GROUP
ATOM O1    OK   -0.424
ATOM C1    CK    0.424
ATOM C2    C3K   0.000
ATOM C3    C2K   0.000
ATOM C4    C2K   0.000
ATOM C5    C3K   0.000
BOND C1 C2 C1 C3 C3 C4 C4 C5
DOUBLE C1 O1
PATCHING FIRS NONE LAST NONE

RESI O2           0.000 ! Oxygen molecule
GROUP
ATOM O21   O2   -0.113
ATOM M1    MO2   0.226
ATOM O22   O2   -0.113
BOND O21 M1 M1 O22
PATCHING FIRS NONE LAST NONE

RESI N2           0.000 ! Nitrogen molecule
GROUP
ATOM N21   N2   -0.482
ATOM Z1    ZO2   0.964
ATOM N22   N2   -0.482
BOND N21 Z1 Z1 N22
PATCHING FIRS NONE LAST NONE

RESI TIP          0.000 ! tip3p water model, generate using noangle nodihedral
GROUP
ATOM OH2  OT     -0.834
ATOM H1   HT      0.417
ATOM H2   HT      0.417
BOND OH2 H1 OH2 H2
!!H1 H2    ! the last bond is needed for shake, but not in NAMD
ANGLE H1 OH2 H2             ! required

END
```

Appendix E: Example VMD Script File Used to Prepare PSF and Final PDB

An example VMD script file is shown in **Table E - 1**; the PDB file that is being modified is the one created using the PACKMOL input file shown in **Table C - 1**.

Table E - 1: VMD script file used to prepare PSF and final PDB files for a Methane-Carbon Dioxide system; the PDB file that is being modified by this script is the one generated with the PACKMOL input file shown in **Table C - 1**.

```
# specify topology file to be used
topology topology_file.inp

# clear structure and load psfgen package
resetpsf
package require psfgen

# separate chains into different PDB files
set chainA [atomselect top "chain A"]
$chainA writepdb chainA.pdb

set chainB [atomselect top "chain B"]
$chainB writepdb chainB.pdb

# create segments and add new segment labels to PDB files
segment MET {pdb chainA.pdb}
segment CO2 {pdb chainB.pdb}

coordpdb chainA.pdb MET
coordpdb chainB.pdb CO2

# create PSF file and final PDB file
writepsf new-mixture.psf
writepdb new-mixture.pdb
```

Appendix F: NAMD Parameter File

Table F - 1: NAMD parameter file used for MD simulations.

```
BONDS
!
!V(bond) = Kb(b - b0)**2
!
!Kb: kcal/mole/A**2
!b0: A
!
!atom type Kb          b0
!
!METHANE
!
!ETHANE
CH3   CH3    3000.00      1.540
!
!BENZENE
ACH   ACH    3000.00      1.400
!
!PROPANE
CH3   CH2    3000.00     1.540
!
!CYCLOHEXANE
CC2   CC2    3000.00     1.540
!
!2-METYLPROPANE
CH3   CH     3000.00     1.540
!
!N-BUTANE
CH2   CH2    3000.00     1.540
!
!DIETHYL ETHER
EH3   EH2    3000.00     1.540
EH2   EO     3000.00     1.410
!
!METHANOL
CH3   AO     3000.00     1.430
AO    HA     3000.00     0.945
!
!ETHANOL
CH2   AO     3000.00     1.430
!
!TIP3
OT   HT    450.000     0.9572
!
!CARBON DIOXIDE
OS   CS     3000.00     1.1600
!
!ACETONE
CK   OK     3000.00     1.2290
CK   C3K    3000.00     1.5200
!
!2-PENTANONE
CK   C2K    3000.00     1.5200
C2K  C2K    3000.00     1.5400
C2K  C3K    3000.00     1.5400
```

```
!
!OXYGEN (O2)
O2   MO2    3000.00     0.6050
!
!NITROGEN (N2)
N2   ZO2    3000.00     0.5500


ANGLES
!
!V(angle) = Ktheta(Theta - Theta0)**2
!
!V(Urey-Bradley) = Kub(S - S0)**2
!
!Ktheta: kcal/mole/rad**2
!Theta0: degrees
!Kub: kcal/mole/A**2 (Urey-Bradley)
!S0: A
!
!atom types     Ktheta    Theta0   Kub     S0
!
!METHANE
!
!ETHANE
!
!PROPANE
CH3  CH2  CH3  62.07  114.0
!
!BENZENE
ACH  ACH  ACH  3000.  120.0
!
!METHANOL
CH3  AO  HA    55.02  108.5
!
!ETHANOL
CH3  CH2 AO    50.05  109.5
CH2  AO  HA    55.02  108.5
!
!2-METHYLPROPANE
CH3 CH CH3  62.07  112.0
!
!N-BUTANE
CH3 CH2 CH2  62.07  114.0
CH2 CH2 CH3  62.07  114.0
!
!N-PENTANE
CH2 CH2 CH2  62.07  114.0
!
!CYCLOHEXANE
CC2 CC2 CC2  62.07  114.0
!
!DIETHYL ETHER
EH3 EH2 EO  49.95  112.0
EH2 EO  EH2 59.98  112.0
!EO  EH2 EH3 49.95  112.0
!
!TIP3
HT   OT   HT     55.000   104.5200
!
!CARBON DIOXIDE
OS   CS   OS  3000.  180.0
```

```
!
!ACETONE
OK   CK   C3K  62.07  121.4
C3K  CK   C3K  62.07  117.2
!
!2-PENTANONE
C3K  CK   C2K  62.07  117.2
OK   CK   C3K  62.07  121.4
CK   C2K  C2K  62.07  114.0
OK   CK   C2K  62.07  121.4
C2K  C2K  C3K  62.07  114.0
!
!OXYGEN (O2)
O2   MO2   O2  3000.  180.0
!
!NITROGEN (N2)
N2   ZO2   N2  3000.  180.0


DIHEDRALS
!
!V(dihedral) = Kchi(1 + cos(n(chi) - delta))
!
!Kchi: kcal/mole
!n: multiplicity
!delta: degrees
!
!atom types             Kchi    n   delta
!
!METHANE
!
!ETHANE
!
!PROPANE
!
!BENZENE
ACH ACH ACH ACH  0.00 0 0.00
ACH ACH ACH ACH  0.00 1 0.00
ACH ACH ACH ACH  0.00 2 180.00
ACH ACH ACH ACH  0.00 3 0.00
!
!2-METHYLPROPANE
!
!N-BUTANE
CH3 CH2 CH2 CH3  0.00 0 0.00
CH3 CH2 CH2 CH3  0.71 1 0.00
CH3 CH2 CH2 CH3 -0.14 2 180.00
CH3 CH2 CH2 CH3  1.57 3 0.00
!
!ETHANOL
CH3 CH2 AO  HA   0.00 0 0.00
CH3 CH2 AO  HA   0.42 1 0.00
CH3 CH2 AO  HA  -0.06 2 180.00
CH3 CH2 AO  HA   0.37 3 0.00
!
!CYCLOHEXANE
CC2 CC2 CC2 CC2 10.08 0 0.00
CC2 CC2 CC2 CC2 13.59 1 0.00
CC2 CC2 CC2 CC2  6.97 2 180.00
CC2 CC2 CC2 CC2  0.13 3 0.00
!
```

```
!N-PENTANE
CH3 CH2 CH2 CH2  0.00 0 0.00
CH3 CH2 CH2 CH2  0.71 1 0.00
CH3 CH2 CH2 CH2 -0.14 2 180.00
CH3 CH2 CH2 CH2  1.57 3 0.00
!CH2 CH2 CH2 CH3  0.00 0 0.00
!CH2 CH2 CH2 CH3  0.71 1 0.00
!CH2 CH2 CH2 CH3 -0.14 2 180.00
!CH2 CH2 CH2 CH3  1.57 3 0.00
!
!DIETHLY ETHER
!EH3 EH2 EO EH2  0.00 0 0.00
!EH3 EH2 EO EH2  1.44 1 0.00
!EH3 EH2 EO EH2 -0.33 2 180.00
!EH3 EH2 EO EH2  1.11 3 0.00
EH2 EO EH2 EH3  0.00 0 0.00
EH2 EO EH2 EH3  1.44 1 0.00
EH2 EO EH2 EH3 -0.33 2 180.00
EH2 EO EH2 EH3  1.11 3 0.00
!
!2-PENTANONE
C3K CK  C2K C2K -0.03 0 0.00
C3K CK  C2K C2K  1.49 1 0.00
C3K CK  C2K C2K  0.03 2 180.00
C3K CK  C2K C2K  0.56 3 0.00
!
CK  C2K C2K C3K  0.00 0 0.00
CK  C2K C2K C3K  0.71 1 0.00
CK  C2K C2K C3K -0.14 2 180.00
CK  C2K C2K C3K  1.57 3 0.00
!
C2K C2K CK  OK   4.04 0 0.00
C2K C2K CK  OK  -1.46 1 0.00
C2K C2K CK  OK   0.11 2 180.00
C2K C2K CK  OK  -0.58 3 0.00
!
!CARBON DIOXIDE
!
!ACETONE
!
!OXYGEN
!
!NITROGEN
!


IMPROPER
!
!V(improper) = Kpsi(psi - psi0)**2
!
!Kpsi: kcal/mole/rad**2
!psi0: degrees
!note that the second column of numbers (0) is ignored
!
!atom types           Kpsi                   psi0
!


NONBONDED
!
!V(Lennard-Jones) = Eps,i,j[(Rmin,i,j/ri,j)**12 - 2(Rmin,i,j/ri,j)**6]
```

```
!
!epsilon: kcal/mole, Eps,i,j = sqrt(eps,i * eps,j)
!Rmin/2: A, Rmin,i,j = Rmin/2,i + Rmin/2,j
!
!atom  ignored    epsilon      Rmin/2   ignored   eps,1-4       Rmin/2,1-4
!
!traPPE CH4
CH4     0.000000  -0.293961     2.093392
!
!traPPE CH3
CH3     0.000000  -0.194650     2.104616
!
!traPPE CH2
CH2     0.000000  -0.091366     2.216863
!
!traPPE CH
CH     0.000000  -0.019862     2.626561
!
!traPPE C
C     0.000000  -0.000993     3.591879
!
!TIP3 HYDROGEN
HT     0.000000  -0.046000     0.224500
!TIP2 OXYGEN
OT     0.000000  -0.152100     1.768200
!
!traPPE small CO2 OXYGEN
OS     0.000000  -0.156912     1.711755
!
!traPPE small CO2 CARBON
CS     0.000000  -0.053628     1.571447
!traPPE UA ketone
CK     0.000000  -0.079449     2.143903
C2K    0.000000  -0.091366     2.216863
C3K    0.000000  -0.194650     2.104616
OK     0.000000  -0.156912     1.711755
!
!traPPE small O2 OXYGEN
O2     0.000000  -0.097325     1.694918
!
!traPPE small O2 M (dummy)
MO2    0.000000  0.000000     0.000000
!
!traPPE small N2 OXYGEN
N2     0.000000  -0.071504     1.857675
!
!traPPE small N2 Z (dummy)
ZO2    0.000000  0.000000     0.000000
!
!traPPE UA Ethers CH3
EH3     0.000000  -0.194650     2.104616
!
!traPPE UA Ethers CH2
EH2     0.000000  -0.091366     2.216863
!
!traPPE UA Ethers O
EO      0.000000  -0.109242     1.571447
!
!traPPE UA Alcohols O
AO      0.000000  -0.184719     1.694918
!
```

```
!traPPE UA Alcohols H
HA      0.000000  -0.000000     0.000000
!
!traPPE UA Cyclic Alkanes CC2
CC2     0.000000  -0.104277     2.194413
!
!traPPE UA Aromatics ACH
ACH     0.000000  -0.100304     2.073749

END
```

Appendix G: Example NAMD Configuration Files

Table G - 1: NAMD configuration file used to simulate a Methane system for estimating self-diffusion at 400 K and 1 atm.

```
#############################################################
## ADJUSTABLE PARAMETERS                                   ##
#############################################################

structure          new-mixture.psf
coordinates        new-mixture.pdb
set temperature    400.
set outputname     methane_methane
firsttimestep      0

#############################################################
## SIMULATION PARAMETERS                                   ##
#############################################################

# Input
paraTypeCharmm     on
parameters          parameter_file.inp
temperature         $temperature

# Center of Mass Motion
COMmotion           no

# Force-Field Parameters
exclude             1-4
#1-4scaling          1.0
cutoff              14.0
switching           on
switchdist          12.0
pairlistdist        16.0

# Integrator Parameters
timestep            2.0  ;# 2fs/step
rigidBonds          all  ;# needed for 2fs steps
nonbondedFreq       1
fullElectFrequency  2
stepspercycle       10

# Constant Temperature Control
langevin            on    ;# do langevin dynamics
langevinDamping     1     ;# damping coefficient (gamma) of 1/ps
langevinTemp        $temperature
langevinHydrogen    off    ;# don't couple langevin bath to hydrogens

# Periodic Boundary Conditions
cellBasisVector1    100.0   0.0   0.0
cellBasisVector2     0.0  100.0   0.0
cellBasisVector3     0.0    0   1106.0
cellOrigin          0.0   0.0   0.0

wrapWater           off              ;# wrap water to central cell
wrapAll             off              ;# wrap other molecules too
```

```
#PME (for full-system periodic electrostatics)
PME                 yes

# let NAMD determine grid
PMEGridSpacing      1.0

# Output
outputName          $outputname

restartfreq         100     ;# 500steps = every 1ps
dcdfreq             100
velDCDfreq          100
xstFreq             100
outputEnergies      100
outputPressure      100


#############################################################
## EXECUTION SCRIPT                                        ##
#############################################################

# Minimization
minimize            1000
reinitvels          $temperature
run 1000000 ;# 2ns
```

Table G - 2: NAMD configuration file used to simulate a Methane-Carbon Dioxide system for estimating binary gas diffusion at 298 K and 1 atm.

```
#############################################################
## ADJUSTABLE PARAMETERS                                   ##
#############################################################

structure          new-mixture.psf
coordinates        new-mixture.pdb
set temperature    298.
set outputname     methane_co2
firsttimestep      0

#############################################################
## SIMULATION PARAMETERS                                   ##
#############################################################

# Input
paraTypeCharmm     on
parameters          parameter_file.inp
temperature         $temperature

# Center of Mass Motion
COMmotion           no

# Force-Field Parameters
exclude             1-4
#1-4scaling          1.0
cutoff              14.0
switching           on
switchdist          12.0
pairlistdist        16.0

# Integrator Parameters
timestep            2.0  ;# 2fs/step
rigidBonds          all  ;# needed for 2fs steps
nonbondedFreq       1
fullElectFrequency  2
stepspercycle       10

# Constant Temperature Control
langevin            on    ;# do langevin dynamics
langevinDamping     1     ;# damping coefficient (gamma) of 1/ps
langevinTemp        $temperature
langevinHydrogen    off    ;# don't couple langevin bath to hydrogens

# Periodic Boundary Conditions
cellBasisVector1    100.0   0.0   0.0
cellBasisVector2     0.0  100.0   0.0
cellBasisVector3     0.0    0   1093.0
cellOrigin          0.0   0.0   0.0

wrapWater           on              ;# wrap water to central cell
wrapAll             on              ;# wrap other molecules too
```

```
#PME (for full-system periodic electrostatics)
PME                 yes

# let NAMD determine grid
PMEGridSpacing      1.0

# Output
outputName          $outputname
restartfreq         100     ;# 500steps = every 1ps
dcdfreq             100
velDCDfreq          100
xstFreq             100
outputEnergies      100
outputPressure      100

#############################################################
## EXECUTION SCRIPT                                        ##
#############################################################

# Minimization
minimize            1000
reinitvels          $temperature
run 1000000 ;# 2ns
```

Table G - 3: NAMD configuration file used to simulate evaporation of Diethyl Ether in Air at 296 K and 1 atm.

```
#############################################################
## ADJUSTABLE PARAMETERS                                   ##
#############################################################

structure          new-mixture.psf
coordinates        new-mixture.pdb
set temperature    296.
set outputname     ether_air
firsttimestep      0

#############################################################
## SIMULATION PARAMETERS                                   ##
#############################################################

# Input
paraTypeCharmm     on
parameters          parameter_file.inp
temperature         $temperature

# Center of Mass Motion
COMmotion           no

# Force-Field Parameters
exclude             1-4
#1-4scaling          1.0
cutoff              14.0
switching           on
switchdist          12.0
pairlistdist        16.0

# Integrator Parameters
timestep            0.5  ;# 0.5fs/step
rigidBonds          all  ;# needed for 2fs steps
nonbondedFreq       1
fullElectFrequency  2
stepspercycle       10

# Constant Temperature Control
langevin            on    ;# do langevin dynamics
langevinDamping     1     ;# damping coefficient (gamma) of 1/ps
langevinTemp        $temperature
langevinHydrogen    off    ;# don't couple langevin bath to hydrogens

# Periodic Boundary Conditions
cellBasisVector1    33.0   0.0   0.0
cellBasisVector2     0.0  33.0   0.0
cellBasisVector3     0.0    0   7734.0
cellOrigin          0.0   0.0   3867.0

wrapWater           on              ;# wrap water to central cell
wrapAll             on              ;# wrap other molecules too
```

```
#PME (for full-system periodic electrostatics)
PME                 yes

# let NAMD determine grid
PMEGridSpacing      1.0

# Output
outputName          $outputname

restartfreq         400     ;# 2000steps = every 1ps
dcdfreq             400
velDCDfreq          400
xstFreq             400
outputEnergies      400
outputPressure      400

#############################################################
## EXECUTION SCRIPT                                        ##
#############################################################

# Minimization
minimize            1000
reinitvels          $temperature
run 10000000 ;# 5ns
```

Appendix H: Example VMD Script Files for Trajectory Analysis

Table H - 1: VMD script file used to estimate the single particle mean square displacement for a pure substance.

```
# Algorithm for calculating MSD (single particle) for Pure Substance

# Specify output file
set outfile [open "msd_sp.dat" w]

# Set molecules
set molecule1 0

# Time step used for simulation
set TimeStep 2.0e-15

# Steps per frame
set FrameSteps 100.

# Get number of frames
set nf [molinfo $molecule1 get numframes]

# Print labels
puts $outfile "Frame Time_Delay MSD"

# Time Start
set TimeStart 1

# Time Origin Increment
set TimeIncrement 10

# Starting Time Delay
set StartingTimeDelay 1000

# Time Delay Increment
set TimeDelayIncrement 500

# Loop over time delays
for {set k $StartingTimeDelay} {$k < $nf} {incr k $TimeDelayIncrement} {

# Number of time origins available for given time delay
set T_origins [expr ($nf-$k+1)]

# Initialize MSD_sp
set MSD_sp 0.0

set TimeOrigins [expr {($T_origins - $TimeStart+1)/$TimeIncrement}]

# Loop over time origins
for {set i $TimeStart} {$i < [expr ($nf-$k+1)]} {incr i $TimeIncrement} {

# Create two atom selections
# Specify different frames for the two atom selections
# One at the time origin, the other at time origin plus time delay
```

```
set sel1 [atomselect $molecule1 "name OH2 and resname TIP" frame [expr $i-1]]

set sel2 [atomselect $molecule1 "name OH2 and resname TIP" frame [expr $i-1+$k]]

set coord1 [$sel1 get {x y z}]

set coord2 [$sel2 get {x y z}]

# Number of atoms in selection
set N_atoms [$sel1 num]

foreach coord1 $coord1 coord2 $coord2 {

# Mean square displacement for given time delay over all time origins and atoms
set MSD_sp [expr $MSD_sp + {[veclength2 [vecsub $coord2
$coord1]]/$TimeOrigins/$N_atoms}]

}

# Delete selections
$sel1 delete
$sel2 delete

}

# Write to file:  frame, time, MSD_sp
puts $outfile "$k [expr $k*$FrameSteps*$TimeStep] $MSD_sp"

}

#Close file
close $outfile
```

Table H - 2: VMD script file used to estimate the collective mean square displacement for a Methane-Carbon Dioxide System; the trajectory data being analyzed was generated using the NAMD configuration file in **Table G - 2**.

```
# This file estimates collective mean square displacement for a CH4 and CO2 system

# Output file
set outfile [open "msd_com.dat" w]

# Molecules
set molecule1 0

# Get number of frames
set nf [molinfo $molecule1 get numframes]

# Number of steps per frame
set NS 100

# Time Step
set TS [expr 2.0e-15]

# Print labels
puts $outfile "Frame Time_Delay MSD"

# Loop over time delays
for {set k 1} {$k <= $nf} {incr k 100} {

# Number of time origins
set T_origins [expr $nf-$k+1]

# Estimate collective MSD
set MSD 0.0

# Loop over time origins
for {set i 1} {$i <= [expr ($nf-$k+1)]} {incr i 1} {

# Select ch4 molecules
set ch4_sel1 [atomselect $molecule1 "name C1 and resname MET"]
set ch4_sel2 [atomselect $molecule1 "name C1 and resname MET"]

# Select co2 molecules
set co2_sel1 [atomselect $molecule1 "name C1 and resname CO2"]
set co2_sel2 [atomselect $molecule1 "name C1 and resname CO2"]

# Number of molecules
set N_ch4 [$ch4_sel1 num]
set N_co2 [$co2_sel1 num]
set N_t [expr $N_ch4 + $N_co2]

# Set frame for selection 1
$ch4_sel1 frame [expr $i-1]
$co2_sel1 frame [expr $i-1]

# Set frame for selection 2
$ch4_sel2 frame [expr $i+$k-1]
$co2_sel2 frame [expr $i+$k-1]

# Get center of mass for selections
set ch4_com1 [measure center $ch4_sel1 weight mass]
set co2_com1 [measure center $co2_sel1 weight mass]
```

```
set ch4_com2 [measure center $ch4_sel2 weight mass]
set co2_com2 [measure center $co2_sel2 weight mass]

# Center of mass separation in Z direction
set j1 [expr {[lindex $ch4_com1 2]-[lindex $co2_com1 2]}]
set j2 [expr {[lindex $ch4_com2 2]-[lindex $co2_com2 2]}]

# Define a pre-factor
set PF [expr {double($N_t)*0.5*0.5}]

# Estimate mean square displacement for given time delay
set MSD [expr $MSD + ($PF*($j2-$j1)*($j2-$j1)/double($T_origins))]

# Delete selections
$ch4_sel1 delete
$co2_sel1 delete
$ch4_sel2 delete
$co2_sel2 delete

}

# Write to file
puts $outfile "$k [expr $k*$NS*$TS] [expr $MSD*1.0e-20]"

}

#Close file
close $outfile
```

Table H - 3: VMD script file used to track how a liquid phase sandwiched between layers of Air spreads with time.

```
# This file tracks the center of mass (COM) of liquid molecules in Air

# Output file
set outfile [open "evap1.dat" w]

# Print labels
puts $outfile "Frame Time COM-COM_R COM-COM_L Area"

# Molecules
set molecule1 0

# PDB Velocity Factor, convert to A/ps
set Vfactor 20.45482706

# Steps per Frame
set StepsPerFrame 1600

# Time Step
set TimeStep 0.5e-15

# Number of frames
set nf [molinfo $molecule1 get numframes]

# Unit cell dimensions X, Y, Z
set X [molinfo $molecule1 get {a}]
set Y [molinfo $molecule1 get {b}]
set Z [molinfo $molecule1 get {c}]

# Loop over frames
for {set i 0} {$i <= $nf} {incr i} {

# Center of mass of all liquid molecules
set com_sel1 [atomselect $molecule1 "resname ACE" frame $i]
set COM [lindex [measure center $com_sel1 weight mass] 2]

# Center of mass of liquid molecules with Z > COM
set ACE1_sel1 [atomselect $molecule1 "resname ACE and z>$COM" frame $i]
set N_ACE1 [$ACE1_sel1 num]
set ACE1_COM [lindex [measure center $ACE1_sel1 weight mass] 2]

# Center of mass of liquid molecules with Z < COM
set ACE2_sel1 [atomselect $molecule1 "resname ACE and z<$COM" frame $i]
set N_ACE2 [$ACE2_sel1 num]
set ACE2_COM [lindex [measure center $ACE2_sel1 weight mass] 2]

# Write to file
puts $outfile "$i [expr $i*$StepsPerFrame*$TimeStep] [expr {$ACE1_COM-$COM}] [expr
{$ACE2_COM-$COM}] [expr $X*$Y]"

# Delete selections
$com_sel1 delete
$ACE1_sel1 delete
$ACE2_sel1 delete

}

#Close file
close $outfile
```

Appendix I: Chapman-Enskog Theory

Based on Chapman-Enskog theory, the diffusion coefficient for gases can be estimated using Equation (40), where D_{AB} is the mutual diffusion coefficient of molecules A and B in m^2/s (or self-diffusion coefficient if A and B are the same molecule), T is the absolute temperature in $Kelvin$, M_A and M_B are the molecular weights of molecules A and B in g/mol, P is the pressure in atm, σ_{AB} is the average collision diameter of molecules A and B $\left(\frac{\sigma_A+\sigma_B}{2}\right)$ in $Angstoms$, Ω is the collision integral and is a function of the reduced temperature T_R defined as $\frac{k_b*T}{\varepsilon_{AB}}$, k_b is the Boltzmann constant, and ε_{AB} is the geometric mean of the minimum potential values for molecules A and B $(\sqrt{\varepsilon_A * \varepsilon_B})$. Collision diameters and minimum potential values for relevant chemicals are listed in **Table I - 1**, while values for the collision integral are listed in **Table I - 2**.

$$D_{AB} = \frac{1.858\text{E-}7 * T^{\frac{3}{2}} * \sqrt{\frac{1}{M_A} + \frac{1}{M_B}}}{P * \sigma_{AB}^2 * \Omega(T_R)} \qquad (40)$$

Table I - 1: Chapman-Enskog inputs; collision diameters and minimum potential values for relevant chemicals.

Chemical	**Collision Diameter, σ_i (Angstroms)**	**Minimum Potential, ε_i/k_b (K)**
Acetone	4.600	560.2
Carbon Dioxide	3.941	195.2
Methane	3.758	148.6
Propane	5.118	237.1
Water	2.641	809.1

Table I - 2: Chapman-Enskog inputs; values of the collision integral at various reduced temperatures.

Reduced Temperature $T_R = (k_b * T)/\varepsilon_{AB}$	**Collision Integral $\Omega(T_R)$**
0.30	2.662
0.40	2.318
0.50	2.066
0.60	1.877
0.70	1.729
0.80	1.612
0.90	1.517
1.00	1.439
1.10	1.375
1.30	1.273
1.50	1.198
1.60	1.167

1.65	1.153
1.75	1.128
1.85	1.105
1.95	1.084
2.1	1.057
2.3	1.026
2.5	0.9996
2.7	0.9770
2.9	0.9576
3.3	0.9256
3.7	0.8998
3.9	0.8888
4.0	0.8836
4.2	0.8740
4.4	0.8652
4.6	0.8568
4.8	0.8492
5.0	0.8422
7	0.7896
9	0.7556
20	0.6640
60	0.5596
100	0.5130
300	0.4360

Appendix J: Rate of Spread

Figure J - 1: Spread of DIETHYL ETHER as it evaporates into Air at 296 K and 1 atm; rate of spread can be estimated from the slope of the least-squares line.

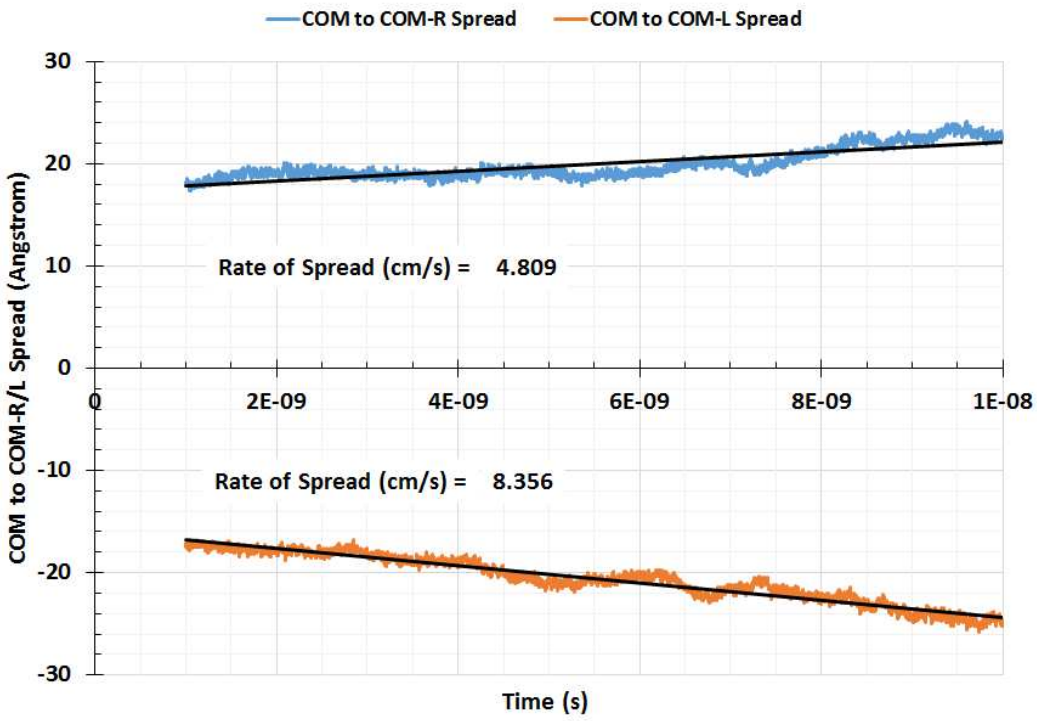

Figure J - 2: Spread of ACETONE as it evaporates into Air at 296 K and 1 atm; rate of spread can be estimated from the slope of the least-squares line.

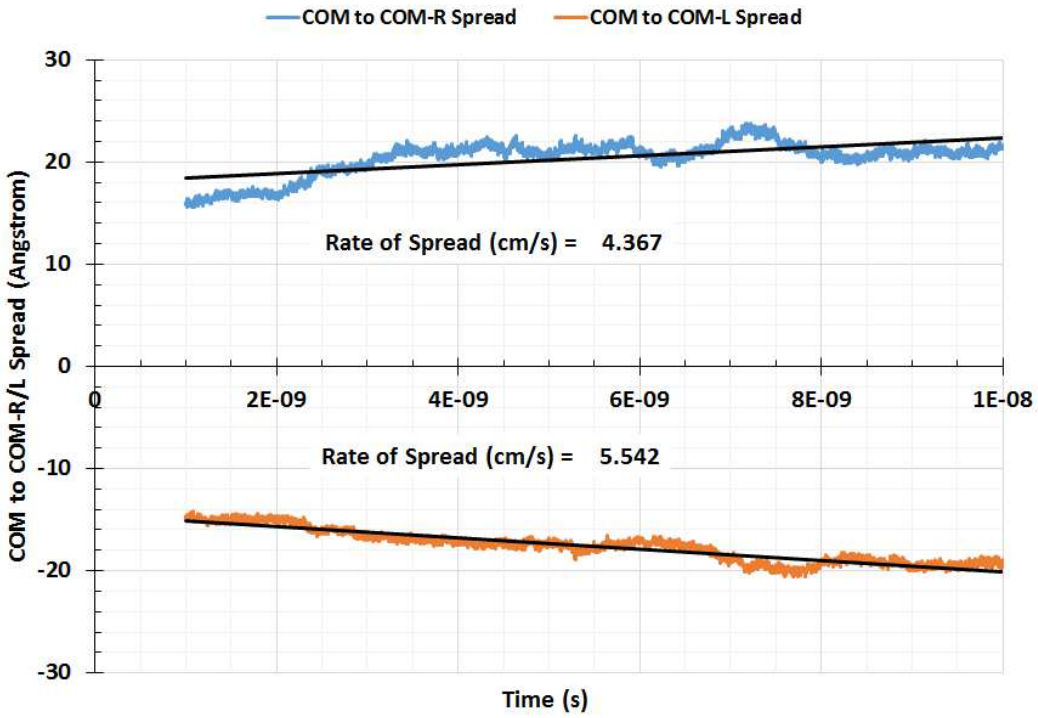

Figure J - 3: Spread of ETHANOL as it evaporates into Air at 296 K and 1 atm; rate of spread can be estimated from the slope of the least-squares line.

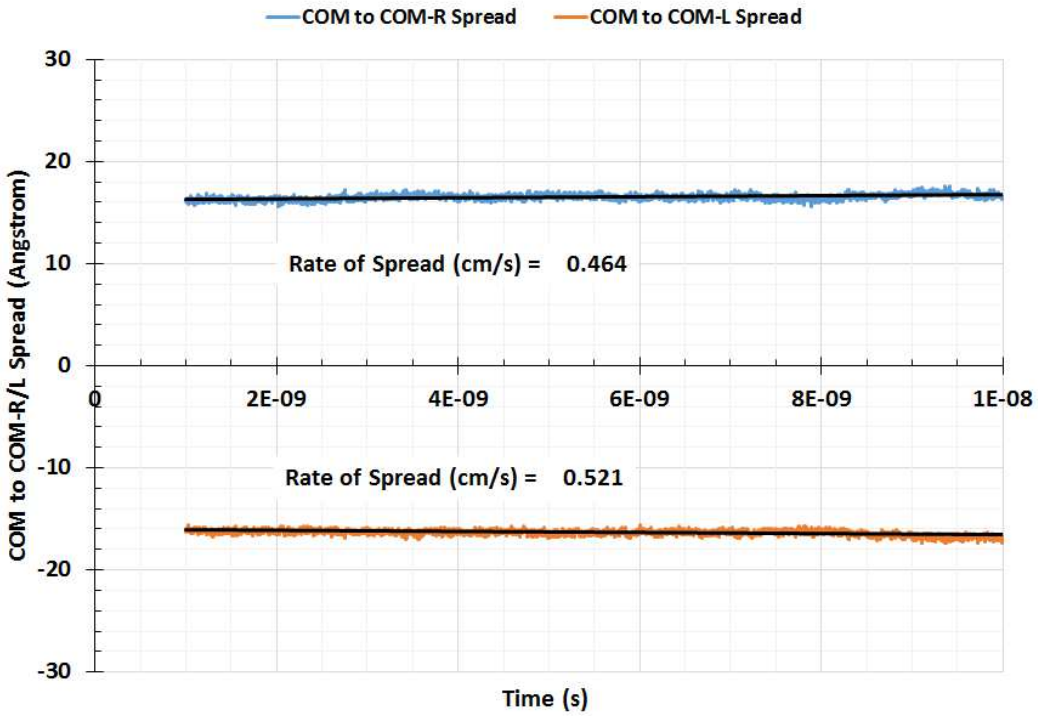

Figure J - 4: Spread of METHANOL as it evaporates into Air at 296 K and 1 atm; rate of spread can be estimated from the slope of the least-squares line.

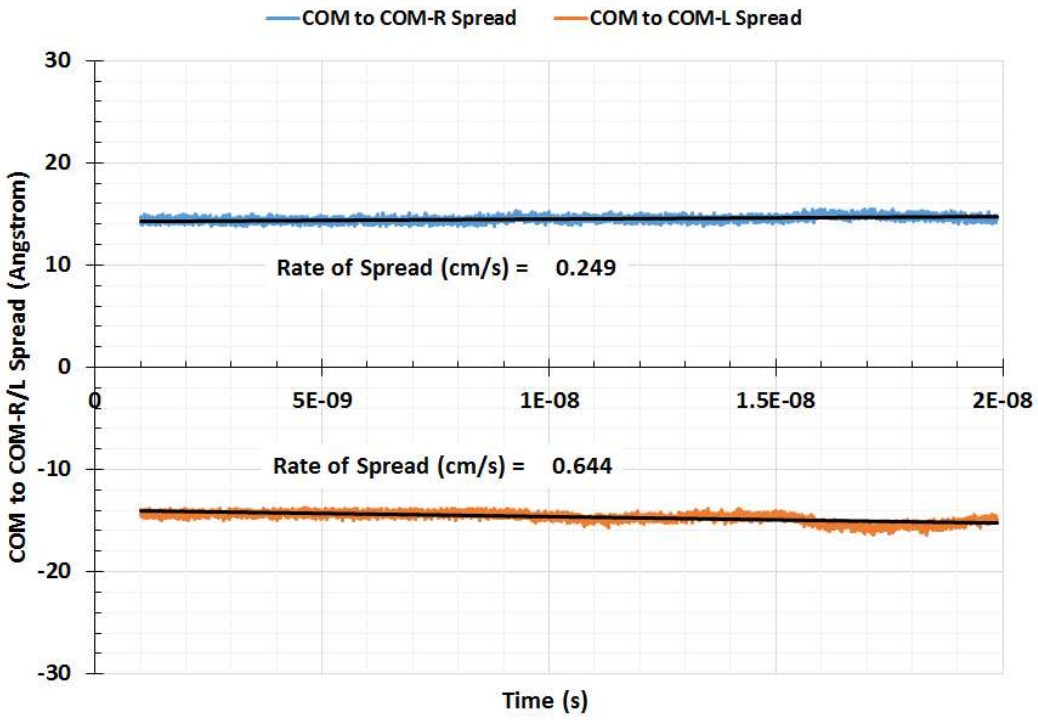

Figure J - 5: Spread of BENZENE as it evaporates into Air at 296 K and 1 atm; rate of spread can be estimated from the slope of the least-squares line.

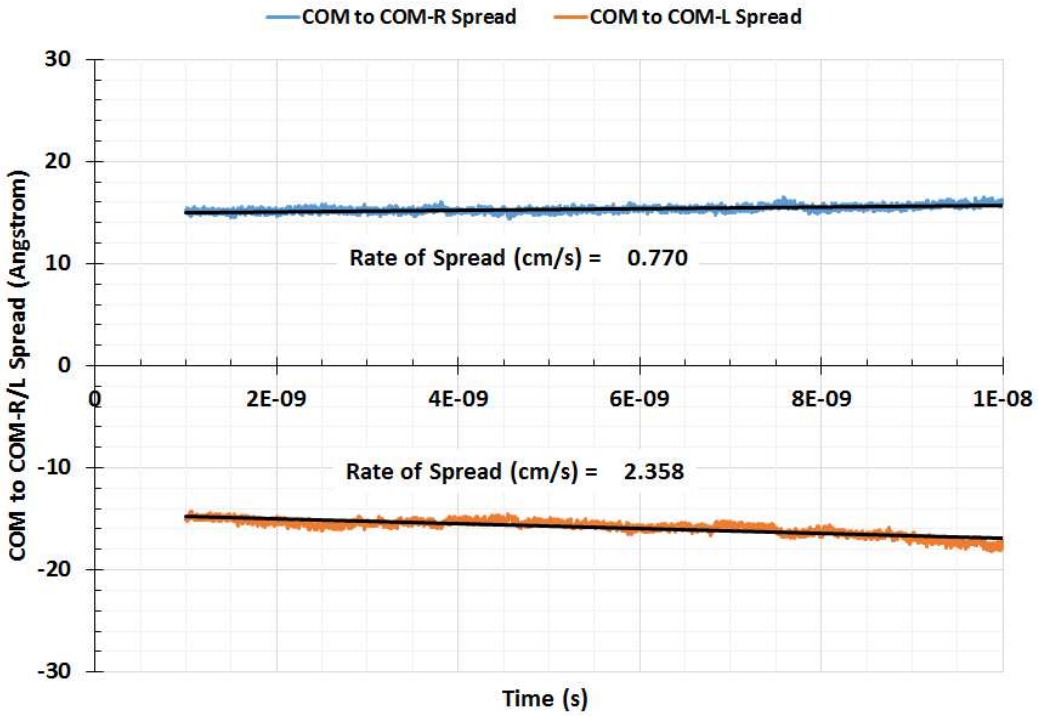

Figure J - 6: Spread of CYCLOHEXANE as it evaporates into Air at 296 K and 1 atm; rate of spread can be estimated from the slope of the least-squares line.

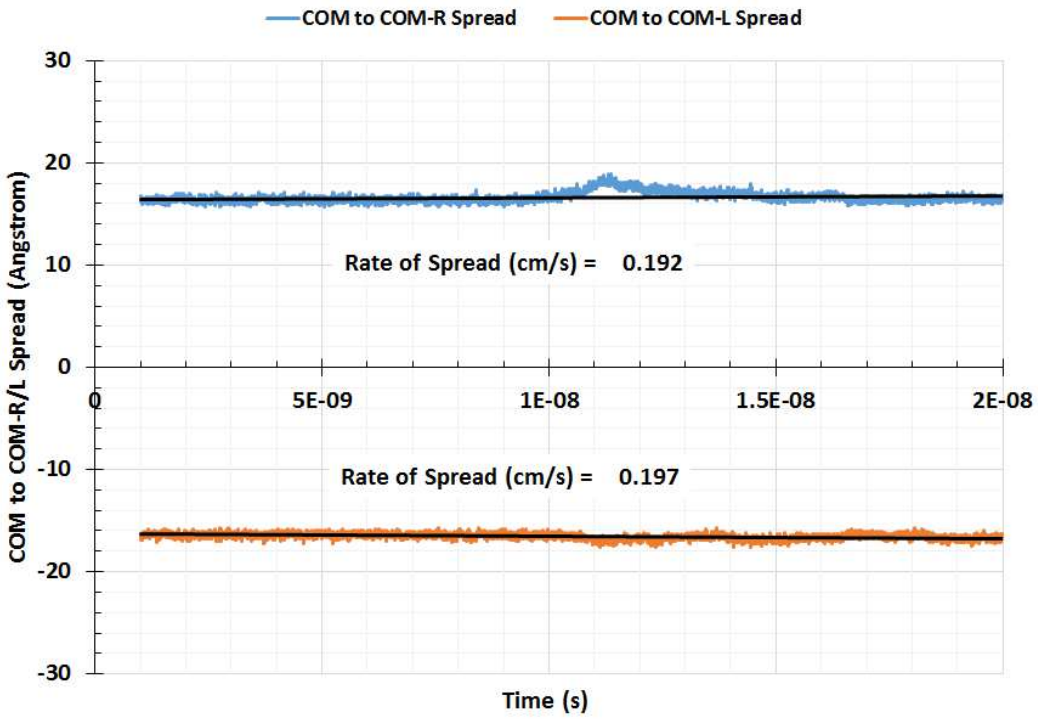

Figure J - 7: Spread of N-PENTANE as it evaporates into Air at 296 K and 1 atm; rate of spread can be estimated from the slope of the least-squares line.

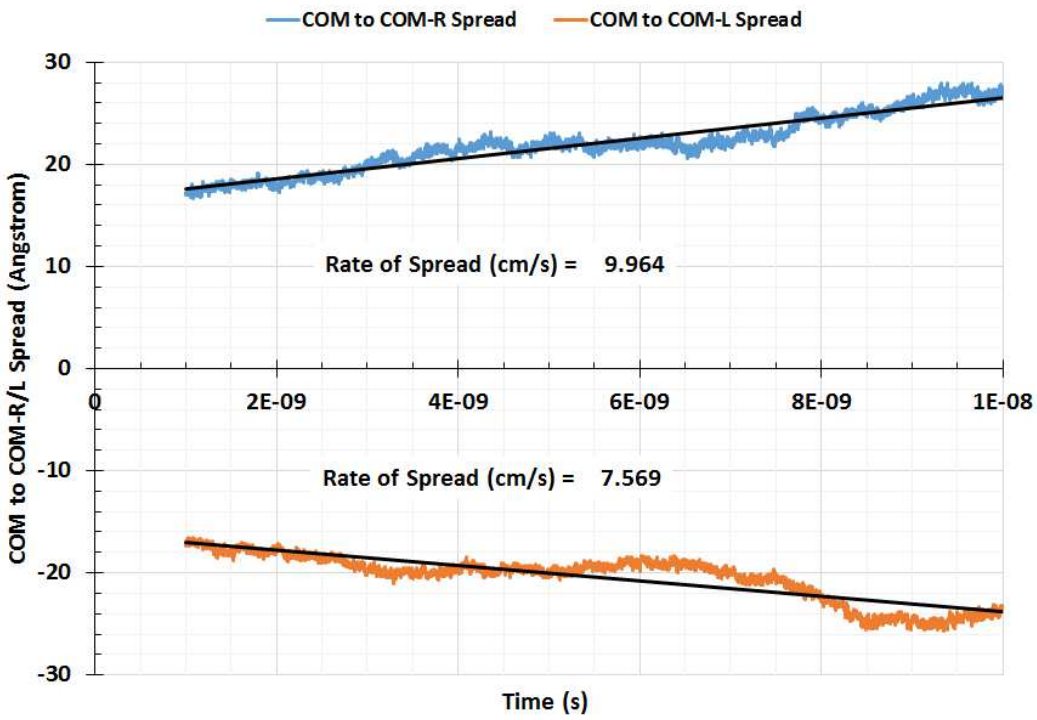

Figure J - 8: Spread of 2-PENTANONE as it evaporates into Air at 296 K and 1 atm; rate fo spread can be estimated from the slope of the least-squares line.

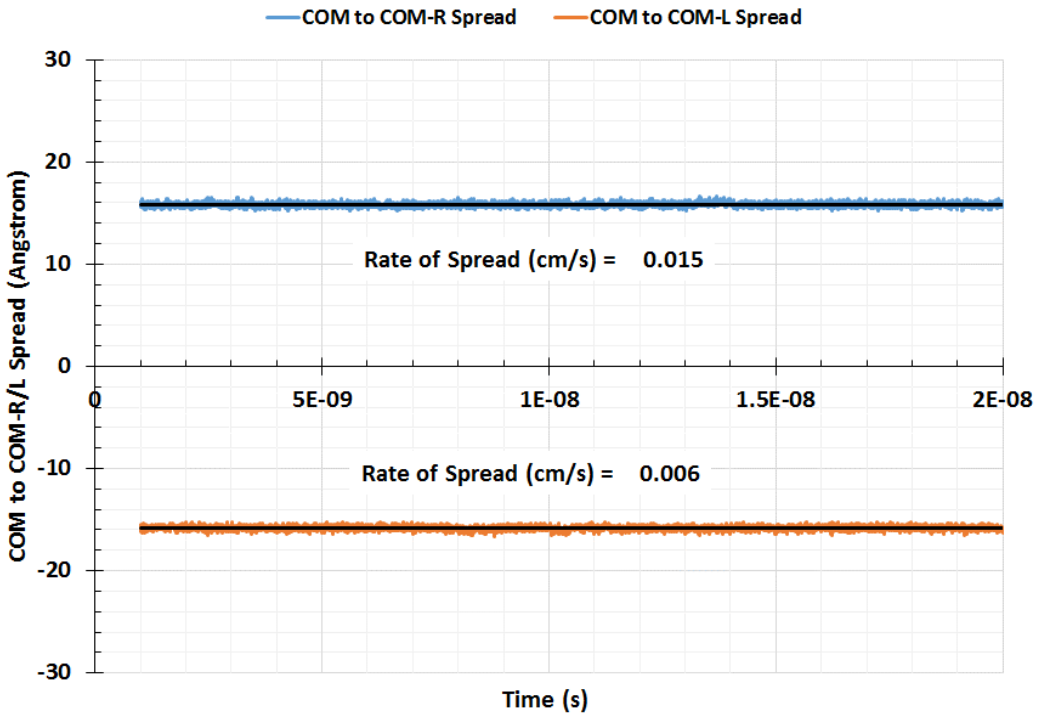

Appendix K: Material Properties for MD Simulations

Table K - 1: The following material properties were used to prepare initial configurations for MD simulation; the density and temperature of these initial configurations correspond approximately to a pressure of 1 atm; T = temperature, P = pressure, ρ = density, MW = molecular weight.

Chemical	MW (g/mol)	ρ (kg/m^3)	T (K)	P (bar)	State	Source
Water	18.0153	0.54761	400	1	gas	(NIST, 2014)
Methane	16.0425	0.4826	400	1	gas	(NIST, 2014)
Carbon Dioxide	44.0095	1.3257	400	1	gas	(NIST, 2014)
Acetone	58.0791	1.7635	400	1	gas	(The Chemistry LibreTexts, 2016)
Propane	44.0956	1.3342	400	1	gas	(NIST, 2014)
Propane	44.0956	1.8085	298	1	gas	(NIST, 2014)
Methane	16.0425	0.64861	298	1	gas	(NIST, 2014)
Carbon Dioxide	44.0095	1.7851	298	1	gas	(NIST, 2014)
Diethyl Ether	74.1216	713.4	298	1	liquid	(NIST, 2014)
Air	28.97	1.184	298	1	gas	(Wikipedia, 2016)
Acetone	58.0791	791	293	1	liquid	(National Center for Biotechnology Information, 2016)
2-Pentanone	86.13	809	298	1	liquid	(Wikipedia, 2016)
n-Pentane	72.15	620.97	298	1	liquid	(NIST, 2014)
Cyclohexane	84.1595	774.03	298	1	liquid	(NIST, 2014)
Benzene	78.1118	873.83	298	1	liquid	(NIST, 2014)
Methanol	32.0419	786.47	298	1	liquid	(NIST, 2014)
Ethanol	46.07	789	293	1	liquid	(Wikipedia, 2016)

Bibliography

Arnold, F. and Engel, A.J. 2001. Evaporation of pure liquids from open surfaces. [book auth.] J.B.H.J. Linders. *Modelling of Environmental Chemical Exposures and Risk.* s.l. : Springer, 2001, pp. 61-71.

Barry, J. 1995. Estimating rates of spreading and evaporation of volatile liquids. *Chemical Engineering Progress.* 1995, pp. 32-39.

Braun, K.O. and Caplan, K.J. 1989. *Evaporation rate of volatile liquids. Final report. Second edition.* Minneapolis : Pace Labs, Inc., 1989.

Chae, K. and Violi, A. 2011. Mutual diffusion coefficients of heptane isomers in nitrogen: A molecular dynamics study. *J. Chem. Phys.* 2011, Vol. 134, 4.

Choudhary, R., Klauda, J.B. 2016. The simultaneous mass and energy evaporation (SM2E) model. *Journal of Occupational and Environmental Hygiene.* 2016, Vol. 13, 4.

Consolini, L., Aggarwal, S.K. and Murad, S. 2003. A molecular dynamics simulation of droplet evaporation. *International Journal of Heat and Mass Transfer.* 2003, Vol. 46.

Cussler, E. L. 2009. *Diffusion: Mass Transfer In Fluid Systems, 3rd edition.* New York : Cambridge University Press, 2009. pp. 118-119. Table 5.1-1; we used the 14 diffusion coefficients in air.

Fehrenbacher, M.C. and Hummel, A.A. 1996. Evaluation of the mass balance model used by the environmental protection agency for estimating inhalation exposure to new chemical substances. *AIHA Journal.* 1996, pp. 526-536.

Fredenslund, A., Jones, R.L. and Prausnitz, J.M. 1975. Group-contribution estimation of activity coefficients in nonideal liquid mixtures. *AIChE Journal.* 1975.

Gajjar, R.M., Miller, M.A. and Kasting, G.B. 2013. Evaporation of volatile organic compounds from human skin in vitro. *Ann. Occup. Hyg.* 2013, pp. 853-865.

Haile, J. M. 1992. *Molecular Dynamics Simulation: Elementary Methods.* New York : Jonh Wiley & Sons, INc., 1992. 0471819662.

Hansen, H.K., et al. 1991. Vapor-liquid equilibria by UNIFAC group contribution. 5. Revision and extension. *Ind. Eng. Chem. Res.* 1991, pp. 2352-2355.

Hummel, A., Braun, K.O. and Fehrenbacher, M.C. 1996. Evaporation of a liquid in a flowing airstream. *AIHA Journal.* 1996, pp. 519-525.

Humphrey, W., Dalke, A. and Schulten, K. 1996. VMD - Visual Molecular Dynamics. *Journal of Molecular Graphics.* 1996, Vol. 14.

Jayjock, M., Armstrong, T. and Taylor, M. 2011. The Daubert standard as applied to exposure assessment modeling using the two-zone (NF/FF) model estimation of indoor air breathing zone conentration as an example. *Journal of Occupational and Environmental Hygiene.* 2011, pp. D114-D122.

Jorgensen, W.L., Chandrasekhar, J. and Madura, J.D. 1983. Comparison of simple potential functions for simulating liquid water. *The Journal of Chemical Physics.* 1983, Vol. 79, 2.

Keil, C.B., Nicas, M. 2003. Predicting room vapor concentrations due to spills of organic solvents. *AIHA Journal.* 2003, pp. 445-454.

Knovel. 2013. *Yaws' Handbook of Antoine Coefficients for Vapor Pressure, 2nd electronic edition.* July 13, 2013.

Leach, A. R. 2001. *Molecular Modelling: Principles and Applications (Second Edition).* New York : Pearson Prentice Hall, 2001. 9780582382107.

Long, L.N., Micci, M.M. and Wong, B.C. 1996. Molecular dynamics simulations of droplet evaporation. *Computer Physics Communications.* 1996, Vol. 96.

Mackay, D. and Matsugu, R.S. 1973. Evaporation rates of liquid hydrocarbon spills on land and water. *The Canadian Journal of Chemical Engineering.* 1973, pp. 434-439.

Makrodimitri, Z.A., Unruh, D.J.M. and Economou, I.G. 2011. Molecular Simulations of Diffusion of Hydrogen, Carbon Monoxide, and Water in Heavy n-Alkanes. *J. Phys. Chem. B.* 2011, Vol. 115.

Martinez, L., et al. 2009. Packmol: A package for building initial configurations for molecular dynamics simulations. *Journal of Computational Chemistry.* 2009, Vol. 30, 13.

Middleman, S. 1998. *An introduction to fluid dynamics: principles of analysis and design.* New York : John Wiley & Sons, Inc., 1998.

—. 1998. *An introduction to mass and heat transfer: principles of analysis and design.* New York : John Wiley & Sons, Inc., 1998.

National Center for Biotechnology Information. 2016. Acetone. *PubChem Compound Database.* [Online] 2016. https://pubchem.ncbi.nlm.nih.gov/compound/acetone.

Nielsen, F., Olsen, E. and Fredunslund, A. 1995. Prediction of isothermal evaporation rates of pure volatile organic compounds in occupational environments - a theoretical approach based on laminar boundary layer theory. *Ann. Occup. Hyg.* 1995, pp. 497-511.

NIST. 2014. NIST Chemistry WebBook. [Online] December 31, 2014. http://webbook.nist.gov/chemistry/.

O'Boyle, N.M., et al. 2011. Open Babel: An open chemical toolbox. *Journal of Cheminformatics.* 2011, Vol. 3.

Okamoto, K., et al. 2010. Evaporation characteristics of multi-component liquid. *Journal of Loss Prevention in the Process Industries.* 2010, pp. 89-97.

Olsen, E. and Nielsen, F. 1995. On the prediction of evaporation rates - with special emphasis on aqueous solutions. *Ann. Occup. Hyg.* 1995, pp. 513-522.

Phillips, J.C., et al. 2005. Scalable molecular dynamics with NAMD. *Journal of Computational Chemistry.* 2005, Vol. 26, 16.

Poling, B.E., Prausnitz, J.M. and O'Connell, J.P. 2001. *The Properties of Gases and Liquids (Fifth Edition).* New York : The McGraw-Hill Companies, Inc., 2001. 0-07-149999-7.

Randhol, P. and Engelien, H.K. 2014. XLUNIFAC version 1.0. *XLUNIFAC.* [Online] December 10, 2014. http://www.pvv.org/~randhol/xlunifac/.

Reinke, P.H., Brosseau, L.M. 1997. Development of a model to predict air contaminant concentrations following indoor spills of volatile liquids. *Ann occup. Hyg.* 1997, pp. 415-435.

Royal Society of Chemistry. 2015. *ChemSpider: Search and share chemistry.* [Online] 2015. http://www.chemspider.com/.

Sawhney, G.S. 2010. *Heat and Mass Transfer, Second Edition.* s.l. : I K International Publishing House, 2010.

Sharma, R., Tankeshwar, K. and Ranganathan, S. 2011. Mass Dependence of Mutual Diffusion Coefficient: Computer Simulation Study. *Physics and Chemistry of Liquids.* 2011, Vol. 49, No. 2.

Smith, J.M., Van Ness, H.C. and Abbott, M.M. 2005. *Introduction to chemical engineering thermodynamics, 7th edition.* Boston : McGraw-Hill, 2005.

Smith, R.L. 2001. Predicting evaporation rates and times for spills of chemical mixtures. *Ann. Occup. Hyg.* 2001, pp. 437-445.

The Chemistry LibreTexts. 2016. A8: van der Waal's Constants for Real Gases. [Online] 2016. http://chem.libretexts.org/Reference/Reference_Tables/Atomic_and_Molecular_Properties/A8%3A_van_der_Waal's_Constants_for_Real_Gases.

The Engineering ToolBox. 2014. Air Properties. *Engineering Tool Box.* [Online] December 31, 2014. http://www.engineeringtoolbox.com/air-properties-d_156.html.

The Siepmann Group. 2015. *TraPPE: Transferable Potentials for Phase Equilibria Force Field.* [Online] 2015. http://chem-siepmann.oit.umn.edu/siepmann/trappe/index.html.

U.S. EPA. 2014. Technology Transfer Network Air Toxics Web site. *Xylenes | Technology Transfer Network Air Toxics Web site.* [Online] December 31, 2014. http://www.epa.gov/ttnatw01/hlthef/xylenes.html.

UNIFAC Consortium. Model Comparison. *UNIFAC Consortium.* [Online] [Cited: July 30, 2015.] http://unifac.ddbst.de/model-comparison.html.

Wikipedia. 2016. 2-Pentanone. [Online] 2016. https://en.wikipedia.org/wiki/2-Pentanone.

—. 2016. Density of air. [Online] 2016. https://en.wikipedia.org/wiki/Density_of_air.

—. 2016. Ethanol. [Online] 2016. https://en.wikipedia.org/wiki/Ethanol.

Wilson, L.D. 1955. Evaporation Rates of Solvents and an Improved Method for their Determination. *Paint, Oil and Chemical Review.* 1955, Vol. 118, 24.

Yang, T.H. and Pan, C. 2005. Molecular dynamics simulation of a thin water layer evaporation and evaporation coefficient. *International Journal of Heat and Mass Transfer.* 2005, Vol. 48.

Yu, J. and Wang, H. 2012. A molecular dynamics investigation on evaporation of thin liquid films. *International Journal of Heat and Mass Transfer.* 2012, Vol. 55.

Zhou, Y. and Miller, G.H. 1996. Green-Kubo Formulas for Mutual Diffusion Coefficients in Multicomponent Systems. *J. Phys. Chem.* 1996, Vol. 100, 13.

Zhou, Z., et al. 2005. A molecular dynamics study of nitric oxide in water: Diffusion and structure. *The Journal of Chemical Physics.* 2005, Vol. 123, 5.

List of Publications

Publications that have appeared in print

- Choudhary, R., Klauda, J.B. The Simultaneous Mass and Energy Evaporation (SM2E) Model. Journal of Occupational and Environmental Hygiene. 2015, pp. 243-253. http://dx.doi.org/10.1080/15459624.2015.1101123